ISSN 0869-5911, Petrology, 2017, Vol. 25, No. 4, pp. 396–418. © Pleiades Publishing, Ltd., 2017.
Original Russian Text © A.A. Tsygankov, G.N. Burmakina, V.B. Khubanov, M.D. Buyantuev, 2017, published in Petrologiya, 2017, Vol. 25, No. 4, pp. 395–418.

Geodynamics of Late Paleozoic Batholith-Forming Processes in Western Transbaikalia

A. A. Tsygankov[a, b, *], G. N. Burmakina[a], V. B. Khubanov[b], and M. D. Buyantuev[a]

[a]*Geological Institute, Siberian Branch, Russian Academy of Sciences, Ulan-Ude, 670047 Russia*

[b]*Buryat State University, Ulan-Ude, 670000 Russia*

**e-mail: tsygan@gin.bscnet.ru*

Received May 23, 2016; in final form, September 30, 2016

Abstract—Isotopic dates newly obtained for the northwestern portion of the Angara–Vitim batholith are consistent with preexisting data on the duration of the Late Paleozoic magmatic cycle: 55–60 Ma (from 325 to 280 Ma). These data also indicate that alkaline mafic magmatism in western Transbaikalia began simultaneously with the transition from crustal granite-forming processes to the derivation of granites of a mixed mantle–crustal nature, with gradual enrichment of the juvenile component in the source of the magmas. Analysis of the currently discussed geodynamic models of Late Paleozoic magmatism shows that a key role in all models of extensive granite-forming processes in the region is assigned to mafic mantle magmas, which can be generated in various geotectonic environments: subduction, delamination, decompression, and a mantle plume. The plume model is most consistent with the intraplate character of the Angara–Vitim batholith. The derivation of the vast volume of granitic material (approximately 1 million km^3) should have required a comparable volume of mafic magma that should have been pooled in the middle crust of the Baikal fold area. However, the density structure of the region does not provide evidence of significant volumes of mafic rocks. This suggests that the mechanism of plume–lithospheric interaction that should have induced extensive crustal melting and the origin of vast granite areas was more complicated than simply conductive melting of crustal protoliths in contact with mafic intrusions.

DOI: 10.1134/S0869591117030043

INTRODUCTION

The Late Paleozoic granitoid province in western Transbaikalia covers an area of approximately 200000 km^2 and is one of the few areas of the Earth (Nédélec et al., 1995; Yarmolyuk et al., 2002; Zhao et al., 2008; Whalen et al., 2006) in which granitoids of various composition were formed simultaneously during a few dozen million years. Most geologists agree that such extensive granite derivation could have been maintained by heat (any perhaps also by material) provided by mafic magmas, with this hypothesis finding support in geological observations and isotopic geochronologic data, which imply that the granitoid and mafic magmatic processes were coeval (Litvinovsky et al., 1993; Tsygankov et al., 2010, 2016b; Litvinovsky et al., 2011). At the same time, the coevality of mantle and crustal magmatic pressures within a single area can also be explained by other geodynamic scenarios, which are described by multiple models suggested for the Late Paleozoic geodynamics of Transbaikalia. In this context, the isotopic age of the magmatic products is of key importance, because any geodynamic reconstructions and models should be consistent with the overall geological evolution of the region.

Until the late 1990s, it was commonly believed that Paleozoic magmatism in this area involved a number of major pulses of magmatic activity (*Karta Magmatiocheskikh Formatsii*..., 1989) that were correlated with certain evolutionary episodes of the fold area (Gordienko, 1987; Wickham et al., 1995; Litvinovsky and Zanvilevich, 1998; Litvinovsky et al., 1999). This paradigm is currently fundamentally revised. Isotopic geochronologic data amassing over the past two decades (Yarmolyuk et al., 1997; Tsygankov et al., 2007b, 2010, 2016a, 2016b; Kovach et al., 2012; Doroshkevich et al., 2012a, 2012b; Khubanov et al., 2016 and references therein) on both the granitoids themselves and the mafic and alkaline rocks led to the practically unanimous consensus that granitoids in western Transbaikalia, including the vast Angara–Vitim batholith (AVB, 150000 km^2 in area), were produced in the Late Paleozoic, but not in the Precambrian or Early Paleozoic, as was believed before (Salop, 1967; Gordienko, 1987; Litvinovsky et al., 1993). In this context, an important problem is the geodynamics of Late Paleozoic batholith-forming processes in Transbaikalia, in view of that some of current interpretations of this issue are diametrically opposite.

We have determined the U–Pb zircon age of granitoids in the northwestern and northern parts of the Angara–Vitim batholith, and our data are consistent with earlier dates that were published in the aforementioned papers. This makes it possible to critically revise current geodynamic models with regard for reliably established geological and isotopic geochronologic constrains.

GEOLOGY

Granitoids of various composition and age make up no less than 80% of the total area of western Transbaikalia. Available data (Yarmolyuk et al., 1997; Tsygankov et al., 2007b, 2010, 2016b; Kovach et al., 2012; Doroshkevich et al., 2012a, 2012b; Khubanov et al., 2016) suggest that the great majority of the rocks was formed in the Late Paleozoic, starting at about 325 Ma and ending at approximately 275 Ma. Granitoid magmatism developed on a heterogeneous Baikalian–Caledonian basement (Bulgatov and Gordienko, 1999; Rytsk et al., 2011; Yarmolyuk et al., 1997) consisting of craton terranes of high-grade metamorphic rocks (Muya, Amalat, Argoda, Garga, and Tsypikan blocks) (Belichenko et al., 2006), ophiolite fragments (Tsygankov, 2005; Kröner et al., 2015), and Riphean and Early Paleozoic island arcs (Tsygankov, 2005; Gordienko et al., 2007, 2010). The central part of the Baikal fold area is believed to be either a Riphean flysch terrane (turbidite basin) (Bulgatov and Gordienko, 1999) or an Early Precambrian Barguzin microcontinent (Zonenshain et al., 1990). The youngest pre-granite complexes are deformed and variably metamorphosed terrigenous–carbonate sediments accumulated in Devonian–Early Carboniferous basins (Ryzhentsev et al., 2012).

Initial Late Paleozoic granitoid magmatism in Transbaikalia (Fig. 1) has produced calc–alkaline granitoids, which are now collectively referred to as the Barguzin Complex (Salop, 1967; Litvinovsky et al., 1993). This complex is typomorphic for the Angara–Vitim batholith (area-pluton). The granitoids of this complex occur over an area of about 150000 km^2. With regard for the average thickness of the granite layer of 10–12 km according to (Litvinovsky et al., 1993) or 5–7 km according to (Turutanov, 2007), this corresponds to a rock volume of some 1–1.5 million km^3, which is comparable with the volume of flood basalts in the Siberian Platform. It is pertinent to mention that the batholith (area–pluton) consists of hundreds of discrete massifs ranging from a few dozen to a few thousand square kilometers in area and consisting of autochthonous gneissose (approximately 20% of the batholith volume) and typical allochthonous (intrusive) equigranular or porphyritic granitoids of similar composition (Litvinovsky et al., 1993; Tsygankov et al., 2010; Litvinovsky et al., 2011). The dominant mafic minerals are biotite in the granites and biotite in association with hornblende in the granodiorites. The foliation of the autochthonous granitoids is parallel to the metamorphic foliation in the host crystalline schists. The marginal portions of the autochthonous gneiss-granite massifs are accompanied by stromatic and venitic migmatites (Reif, 1976), and the inner parts typically host blocks of the host rocks (fragments of the protoliths).

The allochthonous granitoids are equigranular or porphyritic (*Qtz*, *Kfs*) rocks, whose contacts with the host rocks are sharp and which form vein-shaped apophyses in them. The marginal parts of these massifs abound in xenoliths of the host rocks and are locally surrounded by thermal aureoles (Reif, 1976). The granitoids of the Barguzin Complex were formed at approximately 325–290 Ma (Yarmolyuk et al., 1997; Tsygankov et al., 2007b, 2010; Kovach et al., 2012).

Simultaneously with the Barguzin granites and after them, granitoids of two geochemical types were produced at 305–285 Ma: (a) high-K quartz syenites and quartz monzonites (Chivyrkui intrusive complex) and (b) quartz syenites and leucogranites of the Zaza Complex, whose composition is intermediate between high-K calc–alkaline and subalkaline rocks. The typomorphic rocks of the Chivyrkui Complex are porphyritic (*Kfs*) quartz syenite. Some massifs of these rocks are as large as a few hundred square kilometers in area (Litvinovsky et al., 1993). These plutons often consist of several phases and host mingling dikes and mafic microgranular enclaves (MME). For example, the Burgasy Massif in the Ulan-Burgasy Range consists of rocks of three intrusive phases: phase 1 is amphibole–pyroxene and amphibole gabbro, gabbro–monzonite, and monzonite; phase 2 (main) is porphyritic (*Kfs*) quartz syenite (*Hbl*, *Bt*) abounding in MME; and phase 3 is porphyritic (*Qtz*) leucocratic granite porphyry (Burmakina and Tsygankov, 2013).

The Zaza Complex is dominated by equigranular leucocratic biotite granites, which are usually dominant in the two-phase quartz syenite–granite massifs several hundred square kilometers in area.

The emplacement of the massifs of both complexes was associated with the intrusion of subalkaline mafic magmas, which formed relatively small gabbro–monzonite plutons (Orefiev Massif, whose U–Pb zircon age is 290 ± 5 Ma; SHRIMP II), synplutonic bodies of amphibole gabbro (Shaluta Massif, whose Ar–Ar amphibole age is 291.3–289.7), and mingling dikes and mafic enclaves (Litvinovsky et al., 1995; Titov et al., 2000; Tsygankov et al., 2016b; Burmakina and Tsygankov, 2013; Litvinovsky et al., 2012).

Note that the time spans during which the Barguzin, Chivyrkui, and Zaza Complexes were formed significantly overlap, but geological data indicate that in all documented instances they were formed in this exactly sequence, which likely suggest certain relations between the granitoids of various types.

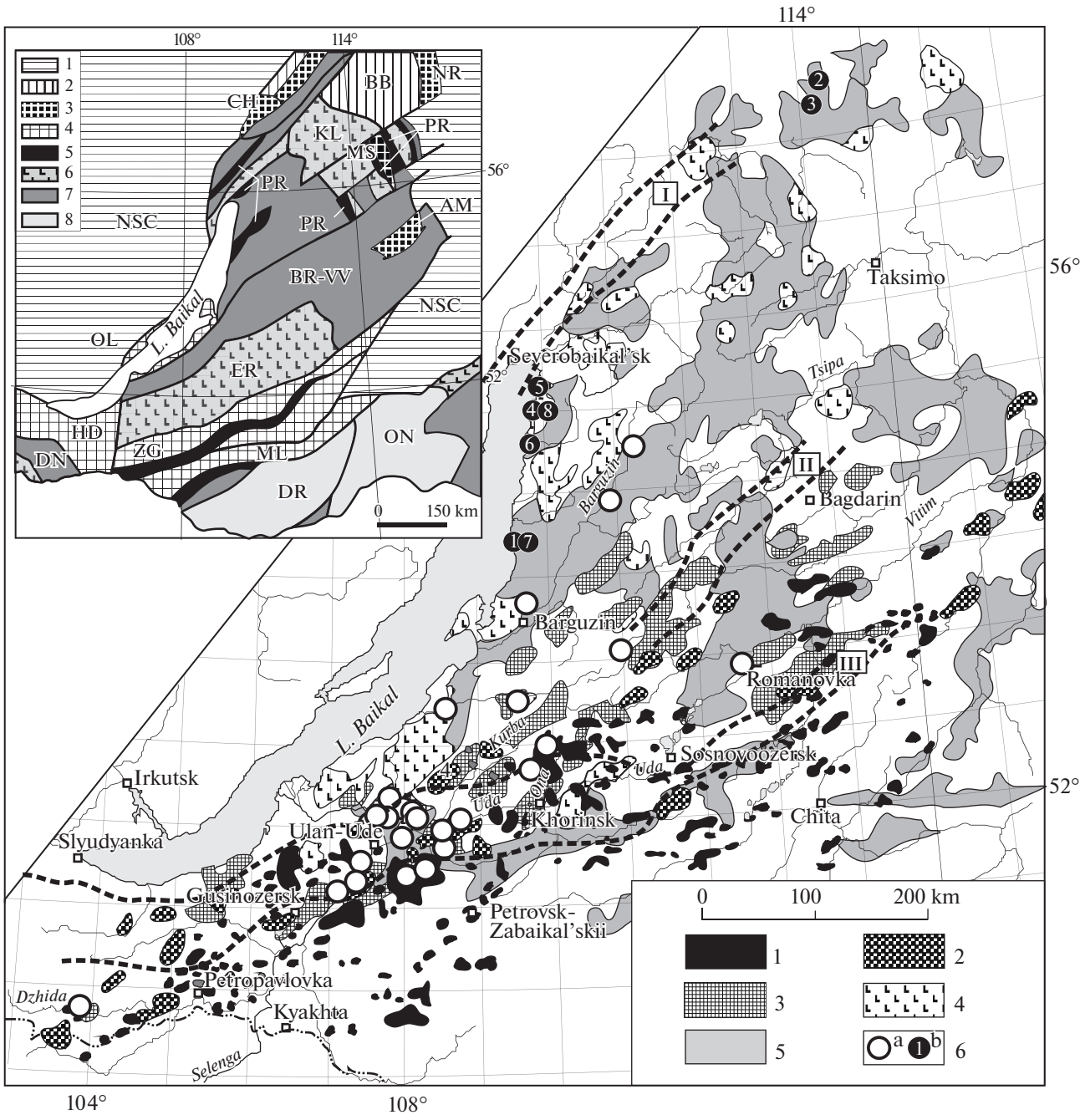

Fig. 1. Schematic map showing the location of Late Paleozoic granitoids in western Transbaikalia (Angara–Vitim batholith) (modified after *Karta magmaticheskikh*..., 1989; Tsygankov et al., 2010). (1) Alkali-feldspar and alkaline granites and syenites of the Mongolian–Transbaikalian volcano-plutonic belt (Early Kunalei Complex, 280–273 Ma) and (Late Kunalei Complex, 230–210 Ma); (2) high-K monzonite–syenite–quartz syenite intrusive series with synplutonic mafic rocks (Lower Selenga Complex, 285–278 Ma); (3) granites transitional from calc–alkaline to alkaline and synplutonic mafic rocks (Zaza Complex, 305–285 Ma); (4) high-K calc–alkaline quartz monzonites, quartz syenites, and gabbroids (Chivyrkui Complex, 305–285 Ma); (5) calc–alkaline auto- and allochthonous granites (Barguzin Complex, 325–290 Ma); (6) sampling sites for U–Pb zircon dating: (a) literature data, (b) this publication (numerals correspond to the sequential numbers of samples in Table 2). Dashed lines show the hypothetical contours of Late Paleozoic rift structures: (I) Synnyr, (II) Saizhen, (III) Uda–Vitim (Yarmolyuk et al., 2014). The inset is a schematic map of terranes in the Baikal fold area (modified after Bulgatov and Gordienko, 1999). (1) North Asian craton (Archean–Early Proterozoic); (2) passive margin of the North Asian craton (Baikal–Patom thrust and fold belt, Late Riphean–Paleozoic); (3) craton terranes (Archean–Early Proterozoic); (4) metamorphic terranes (Early Proterozoic–Paleozoic); (5) oceanic terranes (Early–Middle Riphean, Vendian, Early Cambrian); (6) island arc terranes (Middle–Late Riphean–Early Cambrian) and flysch terranes (turbidite terranes): (7) Early to Middle Riphean–Vendian–Early Cambrian; (8) Devonian–Early Cambrian. NSC—North Asian Craton: CH—Chuya terrane, MS—Muya terrane, AM—Amalat terrane, NR—Necher terrane; passive margin: BB—Bodaibo terrane; metamorphic: HD—Khamar-Daban terrane, Ol—Ol'khon terrane, ML—Malkhan terrane, ZG—Zagan terrane; oceanic: PR—Param terrane; island arc: ER—Eravna terrane, KL—Kelyan terrane, DN—Dzhida terrane; turbidite: BR-VV—Barguzin–Upper Vitim terrane, DR—Dauria terrane, ON—Onon terrane.

The period of time from 285 to 278 Ma was marked by the emplacement of the high-K monzonite–syenite–quartz syenite intrusive series (referred to as the Lower Selenga Complex), accompanied by high-K gabbroids and mingling dikes (the mafic and salic components of a mingling dike have U–Pb zircon ages of 282 ± 5.6 and 281 ± 3.8 Ma, respectively, LA-ICP-MS) (Litvinovsky et al., 1995; Tsygankov et al., 2016b). The typomorphic rocks of this series are monzonitoids and syenites (*Bt*, *Hbl* , and *Px*), which evolve to quartz syenites and subalkaline granites (Tsygankov, 2014). Some of the plutons, for example, the Khasurta Massif, are as large as 900 km^2 (Reif, 1976). The rocks of this massif cut across the Cambrian terrigenous–carbonate rocks transformed (depending on their composition) into apodolomitic spinel–fassaite skarn or plagioclase–quartz–biotite–cordierite hornfels developing after amphibole–biotite schists (Tsygankov et al., 2007a).

The Late Paleozoic magmatic cycle ended with the origin of alkali feldspathic (*Afs*) and alkaline (*Pa*) granites and syenites of the Early Kunalei Complex, whose U–Pb age is 280–273 Ma (Litvinovsky et al., 2002; Reichow et al., 2010). In this complex, detailed data were obtained on the large multiphase Bryan' (1600 km^2) and Khorin (2000 km^2) volcano-plutonic complexes of subalkaline and alkaline plutonic series. Each of them is subdivided into syenite (alkali feldspathic) and alkaline granite stages (Litvinovsky et al., 2002; 2011). During the older stage, AFS syenites dominated over PA granites (in the proportion 9 : 1), whereas this ratio during the late stage was close to 1 : 1. The origin of the alkaline granitoid plutons was predated by the emplacement of dikes of a bimodal trachybasalt–trachyte–trachyrhyolite series, which form a long (approximately 200 km) belt (Khubanov, 2009), and eruptions of trachydacite–trachyrhyolite and trachybasalt–comendite lavas. Alkaline granitoids and volcanic rocks of analogous composition compose the extended Mongol–Transbaikalian volcanic belt. In the territory of Transbaikalia alone, this belt comprises a few hundred alkaline granite massifs and large volcanic fields of trachybasalt, trachyrhyolites, and comendites. The age of some of them (the Kharitonovka and Malyi Kunaley massifs and the volcanoes of the Tsagan-Khurtey Formation) is Late Triassic (230–210 Ma; Litvinovsky et al., 2001; Reichow et al., 2010), but the exact volumetric proportions of the rocks of the alkaline granitoid volcano-plutonic associations of the two age groups are still uncertain.

U–Pb ISOTOPIC AGE

Isotopic dates obtained during the past decade and defining the emplacement succession of the granitoids of various types and the overall duration of Late Paleozoic magmatism in Transbaikalia pertain mostly to the central and southwestern parts of the granitoid areas, whereas modern data on the northern part are absent, and those obtained in the 1980s are ambiguous (Tsygankov et al., 2007b and references therein). At the same time, it is far from obvious whether available isotopic geochronologic data can be accurately extrapolated to the northern portion of the granitoid area. To clarify this issue, we have dated (U–Pb zircon) granitoids of various type sampled on the northeastern shore of Lake Baikal and in the northern marginal part of the Angara–Vitim batholith (on the left-hand side of the Vitim River south of the town of Bodaibo).

The U–Pb isotopic geochronologic study of zircons was carried out at the Geological Institute, Siberian Branch, Russian Academy of Sciences, in Ulan-Ude, by laser ablation–magnetic sector-field–inductively coupled plasma–mass spectrometry (LA-SF-ICP-MS) on an Element XR (Thermo Scientific) high-resolution sector-field mass spectrometer. Material for analysis was sampled using an UP-213 (New Wave Research) laser-ablation system. The reader can find a detailed description of the analytical technique and parameters of the procedure in (Khubanov et al., 2016). Simultaneously with the analysis of each zircon sample, standard reference samples 91500 (1065 Ma) (Wiedenbeck et al., 1995) and Plešovice (337 Ma) (Slama et al., 2008) were analyzed as the external standard and reference sample. The age values were calculated from the weighted averages of the $^{206}Pb/^{238}U$ and $^{207}Pb/^{235}U$ isotopic ratios. The analytical errors of these ratios in the reference sample ranged from 1.05 to 2.12% and from 2.53 to 4.61%. The errors of the weighted average values of the concordant age of zircon Plešovice was 0.01–0.88% of its certified age value of 337.13 Ma.

Zircons were analyzed for Hf by a LEO 1430VP (Carl Zeiss, Germany) scanning electron microscope equipped with an INCA Energy 350 (Oxford Instruments Analytical) energy-dispersive spectrometer. The U and Th concentrations were usually lower than the detection limits. The results of our LA-SF-ICP-MS analysis are summarized in Table 1, the concordia plots are shown in Fig. 2, and the chemical compositions of the samples are presented in Table 2.

For our isotopic geochronologic study of granites of the Barguzin Complex, we took a sample of biotite gneiss-granite (sample BG-04) hosting incompletely melted fragments of the metamorphic source rock. The rock was sampled at Chernyi Cape in the eastern shore of Lake Baikal (Fig. 1). Two samples (Km-11 and Km-12) were collected in the northernmost extremity of the Angara–Vitim batholith at approximately 10 and 18 km south of the town of Bodaibo (Fig. 1). The samples are leucocratic gneiss-granite hosting fragments of crystalline schists of the Balaganakh Group, which are oriented conformably with the foliation of the granitoids.

Zircons in sample BG-04 are of two types: (1) pale yellow, often turbid short-prismatic crystals (aspect ratio 2.2–2.8) 120–200 μm long, which contain 1.8–1.9 wt % HfO_2, and (2) transparent pale pinkish long-

Table 1. Results of LA-ICP-MS zircon dating of granitoids from western Transbaikalia

Analytical spot	Isotopic ratios				Rho	Age, Ma				*D*, %
	$^{207}Pb/^{235}U$	±1σ	$^{206}Pb/^{238}U$	±1σ		$^{207}Pb/^{235}U$	±1σ	$^{206}Pb/^{238}U$	±1σ	
Sample BG-04										
1	0.34510	0.04212	0.04657	0.00178	0.31	301.00	31.80	293.40	10.96	2.59
2	0.37629	0.03741	0.04721	0.00165	0.35	324.30	27.60	297.40	10.15	9.05
3	0.34189	0.01899	0.04660	0.00099	0.38	298.60	14.37	293.60	6.07	1.70
4	0.37186	0.02102	0.04671	0.00102	0.39	321.00	15.56	294.30	6.26	9.07
5	0.35041	0.03339	0.04977	0.00144	0.30	305.00	25.11	313.10	8.86	−2.59
6	0.42350	0.03921	0.04701	0.00161	0.37	358.50	27.97	296.10	9.89	21.07
7	0.32016	0.02707	0.04497	0.00130	0.34	282.00	20.82	283.60	8.04	−0.56
8	0.36992	0.03086	0.04898	0.00139	0.34	319.60	22.87	308.20	8.53	3.70
9	0.35762	0.03678	0.04725	0.00159	0.33	310.40	27.51	297.60	9.79	4.30
10	0.34292	0.03727	0.04801	0.00138	0.26	299.40	28.18	302.30	8.50	−0.96
11	0.34736	0.02216	0.04766	0.00115	0.38	302.70	16.70	300.20	7.09	0.83
12	0.34683	0.02119	0.04721	0.00113	0.39	302.30	15.98	297.40	6.95	1.65
13	0.35448	0.02081	0.04673	0.00110	0.40	308.10	15.60	294.40	6.80	4.65
14	0.33821	0.02932	0.04720	0.00140	0.34	295.80	22.25	297.30	8.62	−0.50
15	0.34524	0.03084	0.04695	0.00152	0.36	301.10	23.28	295.80	9.37	1.79
16	0.37640	0.02207	0.04931	0.00118	0.41	324.40	16.28	310.30	7.22	4.54
17	0.36614	0.03581	0.04689	0.00146	0.32	316.80	26.61	295.40	9.01	7.24
18	0.34999	0.04925	0.04478	0.00181	0.29	304.70	37.04	282.40	11.19	7.90
19	0.35927	0.02924	0.04583	0.00131	0.35	311.70	21.85	288.80	8.06	7.93
20	0.33366	0.03912	0.04934	0.00169	0.29	292.40	29.78	310.50	10.38	−5.83
21	0.40473	0.03256	0.04980	0.00141	0.35	345.10	23.54	313.30	8.67	10.15
22	0.38900	0.03442	0.04935	0.00154	0.35	333.60	25.16	310.50	9.43	7.44
23	0.33791	0.01376	0.04818	0.00095	0.48	295.60	10.44	303.30	5.83	−2.54
Sample Km-11										
1	0.35610	0.02832	0.04792	0.00171	0.45	309.30	21.20	301.70	10.51	2.52
2	0.35915	0.02755	0.04944	0.00170	0.45	311.60	20.59	311.10	10.42	0.16
3	0.36941	0.02525	0.05049	0.00160	0.46	319.20	18.72	317.50	9.80	0.54
4	0.35917	0.02413	0.05140	0.00158	0.46	311.60	18.03	323.10	9.68	−3.56
5	0.36254	0.02307	0.04940	0.00145	0.46	314.10	17.19	310.90	8.88	1.03
6	0.36218	0.01981	0.04948	0.00125	0.46	313.80	14.77	311.30	7.71	0.80
7	0.34055	0.01827	0.04942	0.00121	0.46	297.60	13.84	310.90	7.45	−4.28
8	0.34074	0.01817	0.04592	0.00110	0.45	297.70	13.76	289.40	6.80	2.87
9	0.36887	0.01339	0.05128	0.00089	0.48	318.80	9.93	322.40	5.48	−1.12
10	0.35118	0.02013	0.05111	0.00114	0.39	305.60	15.13	321.30	7.00	−4.89
11	0.38244	0.02076	0.04829	0.00106	0.40	328.80	15.25	304.00	6.55	8.16
12	0.34996	0.01457	0.04693	0.00087	0.45	304.70	10.96	295.60	5.34	3.08
13	0.34346	0.01324	0.04646	0.00083	0.46	299.80	10.00	292.80	5.10	2.39
14	0.34854	0.01531	0.04565	0.00089	0.44	303.60	11.53	287.80	5.48	5.49
15	0.36869	0.01436	0.05033	0.00093	0.47	318.70	10.65	316.50	5.68	0.70
16	0.32605	0.01354	0.04670	0.00090	0.46	286.50	10.37	294.20	5.56	−2.62
17	0.36224	0.01696	0.04983	0.00109	0.47	313.90	12.64	313.50	6.71	0.13
18	0.35646	0.01749	0.04819	0.00111	0.47	309.60	13.09	303.40	6.81	2.04
19	0.34499	0.02244	0.04668	0.00131	0.43	300.90	16.94	294.10	8.05	2.31
20	0.32783	0.02023	0.04535	0.00126	0.45	287.90	15.47	285.90	7.74	0.70
21	0.33821	0.02345	0.04568	0.00146	0.46	295.80	17.80	288.00	9.01	2.71
22	0.34315	0.02649	0.04760	0.00164	0.45	299.60	20.02	299.70	10.12	−0.03
23	0.33433	0.02546	0.04567	0.00160	0.46	292.90	19.37	287.90	9.83	1.74
24	0.34295	0.02602	0.04884	0.00173	0.47	299.40	19.67	307.40	10.65	−2.60

Table 1. (Contd.)

Analytical spot	Isotopic ratios				Rho	Age, Ma				*D*, %
	$^{207}Pb/^{235}U$	±1σ	$^{206}Pb/^{238}U$	±1σ		$^{207}Pb/^{235}U$	±1σ	$^{206}Pb/^{238}U$	±1σ	
Sample Km-12										
1	0.37696	0.01171	0.05148	0.00064	0.40	324.80	8.63	323.60	3.92	0.37
2	0.36890	0.01038	0.04977	0.00059	0.42	318.80	7.70	313.10	3.62	1.82
3	0.37355	0.01309	0.05060	0.00069	0.39	322.30	9.68	318.20	4.26	1.29
4	0.39081	0.01519	0.05140	0.00076	0.38	335.00	11.09	323.10	4.66	3.68
5	0.37546	0.00736	0.05053	0.00051	0.51	323.70	5.44	317.80	3.14	1.86
6	0.35807	0.00723	0.04955	0.00051	0.51	310.80	5.40	311.80	3.16	−0.32
7	0.35504	0.00752	0.04948	0.00053	0.51	308.50	5.64	311.40	3.24	−0.93
8	0.34592	0.00777	0.04882	0.00054	0.49	301.60	5.86	307.30	3.30	−1.85
9	0.36671	0.00780	0.05036	0.00054	0.50	317.20	5.79	316.80	3.34	0.13
10	0.36090	0.00808	0.05080	0.00057	0.50	312.90	6.03	319.50	3.52	−2.07
11	0.34648	0.00791	0.04887	0.00056	0.50	302.10	5.96	307.60	3.44	−1.79
12	0.35645	0.00818	0.04854	0.00056	0.50	309.60	6.12	305.60	3.45	1.31
13	0.34586	0.00810	0.04877	0.00057	0.50	301.60	6.11	307.00	3.52	−1.76
14	0.34688	0.00924	0.04849	0.00062	0.48	302.40	6.97	305.20	3.84	−0.92
15	0.36311	0.01047	0.04858	0.00066	0.47	314.50	7.80	305.80	4.06	2.84
16	0.34348	0.01180	0.04761	0.00071	0.43	299.80	8.92	299.80	4.38	0.00
17	0.35578	0.00975	0.05027	0.00068	0.49	309.10	7.30	316.20	4.18	−2.25
18	0.35612	0.01016	0.05039	0.00070	0.49	309.30	7.61	316.90	4.30	−2.40
19	0.36556	0.01072	0.04920	0.00070	0.49	316.40	7.97	309.60	4.30	2.20
Sample BG-07										
1	0.33727	0.00944	0.04865	0.00064	0.47	295.10	7.17	306.20	3.96	−3.63
2	0.35739	0.01688	0.04916	0.00089	0.38	310.30	12.63	309.40	5.45	0.29
3	0.36060	0.00999	0.05046	0.00067	0.48	312.70	7.45	317.40	4.12	−1.48
4	0.37671	0.01682	0.05067	0.00088	0.39	324.60	12.41	318.60	5.39	1.88
5	0.35620	0.01837	0.04771	0.00091	0.37	309.40	13.76	300.40	5.60	3.00
6	0.36742	0.01252	0.04869	0.00073	0.44	317.70	9.30	306.50	4.49	3.65
7	0.38378	0.01676	0.04902	0.00086	0.40	329.80	12.30	308.50	5.27	6.90
8	0.35268	0.01652	0.05032	0.00090	0.38	306.70	12.40	316.50	5.51	−3.10
9	0.38493	0.01806	0.04782	0.00089	0.40	330.70	13.24	301.10	5.46	9.83
10	0.34782	0.00879	0.04800	0.00062	0.51	303.10	6.62	302.20	3.84	0.30
11	0.40238	0.01913	0.05000	0.00093	0.39	343.40	13.85	314.50	5.70	9.19
12	0.34742	0.01486	0.04651	0.00080	0.40	302.80	11.20	293.10	4.93	3.31
13	0.37409	0.01845	0.04764	0.00091	0.39	322.70	13.63	300.00	5.61	7.57
14	0.34296	0.01044	0.04747	0.00068	0.47	299.40	7.90	298.90	4.21	0.17
15	0.34635	0.01122	0.04691	0.00070	0.46	302.00	8.46	295.50	4.32	2.20
16	0.36234	0.01923	0.04999	0.00099	0.37	314.00	14.33	314.50	6.05	−0.16
17	0.35793	0.01008	0.04927	0.00069	0.50	310.70	7.54	310.00	4.25	0.23
18	0.34354	0.02217	0.04782	0.00105	0.34	299.80	16.76	301.10	6.46	−0.43
19	0.34556	0.01590	0.04812	0.00089	0.40	301.40	12.00	303.00	5.50	−0.53
20	0.34935	0.01631	0.04664	0.00089	0.41	304.20	12.27	293.90	5.51	3.50
21	0.33971	0.01420	0.04865	0.00088	0.43	297.00	10.76	306.30	5.38	−3.04
Sample BG-05										
1	0.33041	0.00968	0.04526	0.00064	0.48	289.90	7.39	285.40	3.97	1.58
2	0.32755	0.00943	0.04554	0.00064	0.49	287.70	7.22	287.10	3.97	0.21
3	0.34310	0.01184	0.04611	0.00072	0.45	299.50	8.95	290.60	4.43	3.06
4	0.33828	0.00977	0.04601	0.00066	0.50	295.90	7.41	290.00	4.07	2.03
5	0.32885	0.01081	0.04493	0.00069	0.47	288.70	8.26	283.30	4.23	1.91
6	0.33219	0.01698	0.04614	0.00091	0.39	291.20	12.94	290.80	5.59	0.14
7	0.33077	0.01930	0.04552	0.00100	0.38	290.20	14.72	287.00	6.16	1.11

Table 1. (Contd.)

Analytical spot	Isotopic ratios				Rho	Age, Ma				*D*, %
	$^{207}Pb/^{235}U$	±1σ	$^{206}Pb/^{238}U$	±1σ		$^{207}Pb/^{235}U$	±1σ	$^{206}Pb/^{238}U$	±1σ	
8	0.34779	0.01538	0.04589	0.00087	0.43	303.10	11.58	289.20	5.39	4.81
Sample BG-08										
1	0.32619	0.01353	0.04481	0.00079	0.43	286.70	10.36	282.60	4.89	1.45
2	0.32632	0.01384	0.04611	0.00082	0.42	286.80	10.59	290.60	5.07	−1.31
3	0.32565	0.01126	0.04590	0.00075	0.47	286.20	8.62	289.30	4.60	−1.07
4	0.36582	0.01761	0.04673	0.00092	0.41	316.60	13.09	294.40	5.68	7.54
5	0.33154	0.01620	0.04554	0.00089	0.40	290.70	12.35	287.10	5.51	1.25
6	0.34625	0.01171	0.04571	0.00075	0.49	301.90	8.83	288.20	4.60	4.75
7	0.32226	0.01298	0.04471	0.00079	0.44	283.60	9.97	282.00	4.87	0.57
8	0.35578	0.01368	0.04606	0.00081	0.46	309.10	10.24	290.30	5.02	6.48
9	0.30743	0.01210	0.04573	0.00081	0.45	272.20	9.39	288.20	4.97	−5.55
10	0.36689	0.01614	0.04717	0.00090	0.43	317.30	11.99	297.10	5.57	6.80
11	0.34429	0.01421	0.04703	0.00087	0.45	300.40	10.73	296.20	5.36	1.42
12	0.34760	0.01286	0.04615	0.00081	0.47	302.90	9.69	290.80	5.01	4.16
13	0.36012	0.01452	0.04763	0.00088	0.46	312.30	10.84	300.00	5.42	4.10
14	0.32167	0.01130	0.04599	0.00079	0.49	283.20	8.68	289.80	4.88	−2.28
15	0.35216	0.01474	0.04618	0.00088	0.46	306.30	11.07	291.10	5.41	5.22
16	0.32254	0.01115	0.04642	0.00081	0.50	283.90	8.56	292.50	4.97	−2.94
17	0.35068	0.01239	0.04779	0.00084	0.50	305.20	9.32	300.90	5.19	1.43
18	0.33685	0.01315	0.04786	0.00089	0.48	294.80	9.99	301.40	5.46	−2.19
19	0.34947	0.01439	0.04831	0.00092	0.46	304.30	10.83	304.10	5.68	0.07
20	0.33093	0.01246	0.04655	0.00086	0.49	290.30	9.51	293.30	5.27	−1.02
21	0.32823	0.01408	0.04542	0.00090	0.46	288.20	10.77	286.40	5.55	0.63
22	0.33080	0.01568	0.04422	0.00093	0.44	290.20	11.96	279.00	5.74	4.01
23	0.34509	0.01858	0.04651	0.00106	0.42	301.00	14.03	293.00	6.51	2.73
24	0.32710	0.01866	0.04486	0.00104	0.41	287.30	14.27	282.90	6.44	1.56
Sample BG−04/3										
1	0.30477	0.00924	0.04257	0.00061	0.47	270.10	7.19	268.70	3.76	0.52
2	0.32747	0.01733	0.04363	0.00087	0.38	287.60	13.26	275.30	5.35	4.47
3	0.32147	0.01064	0.04422	0.00066	0.45	283.00	8.17	279.00	4.09	1.43
4	0.31524	0.00928	0.04413	0.00062	0.48	278.20	7.16	278.40	3.84	−0.07
5	0.32024	0.01260	0.04304	0.00071	0.42	282.10	9.69	271.60	4.41	3.87
6	0.31097	0.01168	0.04248	0.00068	0.43	274.90	9.05	268.20	4.22	2.50
7	0.32112	0.01240	0.04269	0.00070	0.42	282.80	9.53	269.50	4.35	4.94
8	0.30633	0.01304	0.04506	0.00076	0.40	271.30	10.14	284.10	4.71	−4.51
9	0.29131	0.00977	0.04301	0.00064	0.44	259.60	7.68	271.50	3.98	−4.38
10	0.31623	0.00917	0.04562	0.00064	0.48	279.00	7.08	287.60	3.95	−2.99
11	0.32687	0.00991	0.04475	0.00065	0.48	287.20	7.58	282.20	4.01	1.77
12	0.32774	0.00981	0.04310	0.00063	0.49	287.80	7.51	272.00	3.88	5.81
13	0.32117	0.01045	0.04448	0.00067	0.46	282.80	8.03	280.50	4.13	0.82
14	0.31728	0.00992	0.04435	0.00065	0.47	279.80	7.65	279.80	4.04	0.00
15	0.32862	0.00983	0.04446	0.00065	0.49	288.50	7.52	280.40	3.99	2.89
16	0.31171	0.00970	0.04374	0.00065	0.48	275.50	7.51	276.00	4.00	−0.18
17	0.32167	0.00949	0.04341	0.00063	0.49	283.20	7.29	273.90	3.91	3.40
18	0.31710	0.01041	0.04314	0.00066	0.47	279.70	8.03	272.30	4.08	2.72
19	0.32421	0.00791	0.04520	0.00061	0.55	285.10	6.07	285.00	3.76	0.04
20	0.30996	0.00951	0.04452	0.00065	0.48	274.10	7.37	280.80	4.01	−2.39
21	0.31326	0.01113	0.04344	0.00070	0.45	276.70	8.61	274.20	4.30	0.91
22	0.30436	0.01063	0.04204	0.00067	0.46	269.80	8.28	265.40	4.15	1.66
23	0.32447	0.01099	0.04349	0.00069	0.47	285.30	8.42	274.40	4.25	3.97
24	0.31196	0.00957	0.04455	0.00067	0.49	275.70	7.40	281.00	4.12	−1.89

Table 1. (Contd.)

Analytical spot	Isotopic ratios				Rho	Age, Ma				*D*, %
	$^{207}Pb/^{235}U$	±1σ	$^{206}Pb/^{238}U$	±1σ		$^{207}Pb/^{235}U$	±1σ	$^{206}Pb/^{238}U$	±1σ	
25	0.30251	0.00980	0.04294	0.00066	0.47	268.40	7.64	271.10	4.09	−1.00
26	0.30289	0.01059	0.04306	0.00069	0.46	268.70	8.25	271.80	4.28	−1.14
27	0.30686	0.00967	0.04327	0.00067	0.49	271.70	7.51	273.10	4.12	−0.51
28	0.31086	0.01190	0.04332	0.00073	0.44	274.80	9.22	273.40	4.54	0.51
29	0.35852	0.01678	0.04451	0.00087	0.42	311.10	12.54	280.70	5.36	10.83
30	0.32006	0.00952	0.04361	0.00066	0.51	281.90	7.33	275.10	4.09	2.47
Sample BG-07/1										
1	0.33535	0.01090	0.04783	0.00067	0.43	293.60	8.29	301.20	4.13	−2.52
2	0.32934	0.01143	0.04714	0.00069	0.42	289.10	8.73	296.90	4.23	−2.63
3	0.37126	0.01253	0.04819	0.00069	0.42	320.60	9.28	303.40	4.26	5.67
4	0.34573	0.01155	0.04862	0.00069	0.42	301.50	8.71	306.10	4.26	−1.50
5	0.33411	0.01153	0.04713	0.00069	0.42	292.70	8.78	296.90	4.22	−1.41
6	0.34382	0.01202	0.04942	0.00072	0.42	300.10	9.08	311.00	4.45	−3.50
7	0.36264	0.01244	0.04863	0.00071	0.43	314.20	9.27	306.10	4.34	2.65
8	0.34309	0.01146	0.04812	0.00069	0.43	299.50	8.66	303.00	4.22	−1.16
9	0.34869	0.01178	0.04796	0.00069	0.43	303.70	8.87	302.00	4.24	0.56
10	0.34555	0.01160	0.04861	0.00070	0.43	301.40	8.76	306.00	4.27	−1.50
11	0.33268	0.01171	0.04610	0.00068	0.42	291.60	8.92	290.50	4.19	0.38
12	0.36559	0.01211	0.04861	0.00069	0.43	316.40	9.00	306.00	4.24	3.40
13	0.33785	0.01128	0.04702	0.00067	0.43	295.50	8.56	296.20	4.13	–0.24
14	0.33828	0.01107	0.04883	0.00069	0.43	295.90	8.40	307.30	4.22	-3.71
15	0.33682	0.01143	0.04621	0.00067	0.43	294.80	8.68	291.20	4.10	1.24
16	0.34396	0.01183	0.04686	0.00068	0.42	300.20	8.94	295.20	4.20	1.69
17	0.33310	0.01113	0.04635	0.00066	0.43	291.90	8.48	292.10	4.07	–0.07
18	0.33620	0.01163	0.04682	0.00068	0.42	294.30	8.84	295.00	4.20	–0.24
19	0.33868	0.01257	0.04705	0.00072	0.41	296.20	9.53	296.40	4.42	–0.07
20	0.34481	0.01287	0.04733	0.00073	0.41	300.80	9.72	298.10	4.46	0.91
21	0.33639	0.01165	0.04731	0.00069	0.42	294.40	8.85	298.00	4.25	−1.21

Rho is the correlation coefficient between the analytical errors in the $^{207}Pb/^{235}U$ and $^{206}Pb/^{238}U$ ratios, and *D* is discordance, $D = (\text{Age } (^{207}Pb/^{235}U)/ \text{Age } (^{206}Pb/^{238}U) - 1) \times 100$.

prismatic crystals (aspect ratio 3–4.5) 520–660 μm long, containing up to 1.54 wt % HfO_2. The concordant isotopic age (based on 23 analytical spots) of the zircons of both types is 299.1 ± 3.4 Ma, MSWD = 3.5 (Fig. 2a).

The gneissose granites of the Barguzin Complex sampled in the northern part of AVB (sample Km-11) host long-prismatic (aspect ratio 1.7–3.6) transparent, almost colorless or slightly grayish zircon grains ranging from 125 to 220 μm in length and containing up to 6.3 wt % HfO_2. The average age value is 303 ± 3.8 Ma, $n = 24$, MSWD = 0.94 (Fig. 2b). Zircons in sample Km-12 are short-prismatic (aspect ratio 1.1–2), pale yellowish pink, slightly turbid, with rutile inclusions, 125–300 μm long, containing no more than 1.4 wt % HfO_2. The concordant age (based on 19 grains) is 312.2 ± 2.3 Ma, MSWD = 0.33 (Fig. 2c).

To date the granitoids of the Chivyrkui Complex, we collected rock samples in the eastern shore of Lake Baikal: (1) in the area of Urbikan Cape, sample BG-05, which is porphyritic (*Kfs*) *Amph–Bt* quartz syenite; and (2) at Turali Cape and the northern shore of Ayaya Bay, samples BG-07 and BG-08, which are *Amph–Bt* quartz monzonites with rare *Kfs* phenocrysts. The leucogranites of the Zaza type were studied in thin veins (0.5–0.7 m thick) cutting the Barguzin leucogranite (sample BG-04/3) and Chivyrkui quartz monzonite (sample BG-07/1). They differ from the most typical granites of the Zaza Complex (Tsygankov et al., 2010) in possessing a finer grained texture because of the small thicknesses of the sampled bodies.

Zircons in the quartz syenite sample from the Chivyrkui Complex (sample BG-05) are dipyramidal crystals 100–175 μm long, whose aspect ratio is 1.5–2.7. The zircon is dark orange, and its grains are practically opaque, host rutile inclusions, and contain approximately 0.5 wt % HfO_2. The concordant U–Pb isotopic age is 287.8 ± 3.2 Ma, $n = 8$, MSWD = 3.2 (Fig. 2e).

The quartz monzonites (sample BG-07) host long-prismatic zircon crystals 130–320 μm long, whose

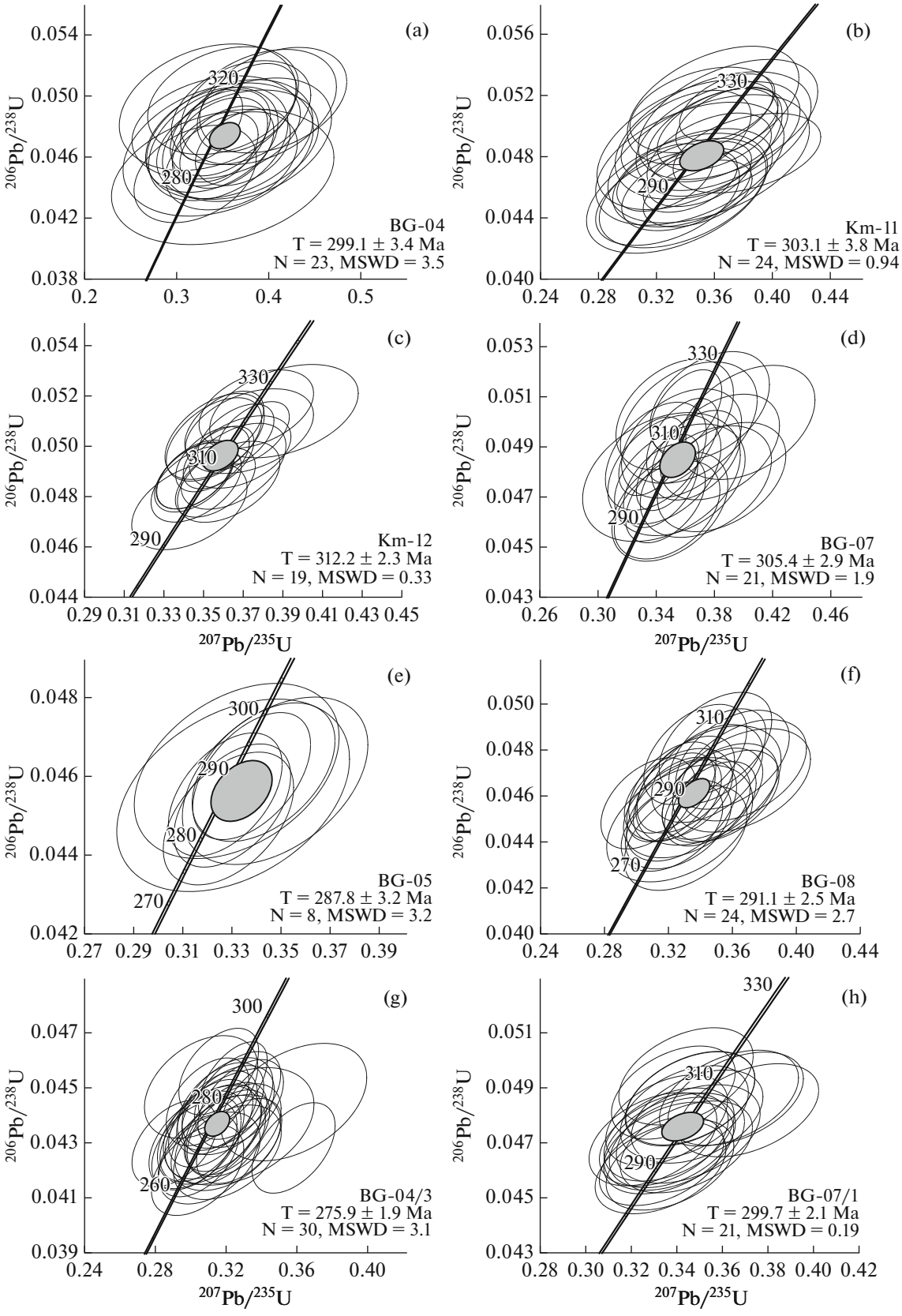

Fig. 2. Concordia plot for zircons from granites of (a–c) the Barguzin and (d–f) Chivyrkui, and (g–h) Zaza complexes in western Transbaikalia. The errors of the U–Pb dates correspond to 95% confidence level (±2σ).

Table 2. Chemical composition of granite samples selected for U–Pb isotopic dating

Component	BG-04	Km-11	Km-12	BG-07	BG-08	BG-05	BG-04/3	BG-07/1
	1	2	3	4	5	6	7	8
SiO_2	77.20	72.70	77.00	62.10	63.50	66.90	74.20	74.50
TiO_2	0.17	0.15	0.04	0.84	0.65	0.47	0.30	0.16
Al_2O_3	12.20	15.10	14.00	15.80	14.90	15.90	13.60	13.50
Fe_2O_3	0.74	0.96	0.39	2.48	1.82	1.95	0.82	0.65
FeO	0.41	0.23	0.15	2.50	2.67	1.13	0.49	0.21
MnO	0.02	0.04	0.02	0.08	0.09	0.06	0.03	0.01
MgO	0.46	0.12	0.10	1.90	2.44	1.02	0.23	0.16
CaO	1.55	0.86	1.02	3.30	3.22	2.43	0.57	0.48
Na_2O	3.89	4.30	4.65	4.30	4.18	4.14	3.37	3.25
K_2O	2.56	4.85	1.78	5.24	4.97	4.90	6.15	6.17
P_2O_5	0.10	0.03	0.03	0.30	0.28	0.17	0.10	0.10
LOI	0.37	0.47	0.48	0.54	0.72	0.53	0.23	0.28
Total	99.57	99.78	99.63	99.38	99.44	99.60	99.99	99.37
Ba	959	1213	469	1290	1113	1462	396	625
Rb	40	180	38	221	200	176	112	261
Sr	229	567	462	612	539	716	89	191
Cs	0.4	1.0	0.8	2.3	3.3	1.3	0.6	1.6
Ga	9.6	20.3	14.3	22.4	19.0	19.0	17.2	17.7
Ta	0.17	0.79	0.28	3.60	2.30	1.93	2.80	2.20
Nb	3.0	15.3	3.8	54.5	31.7	26.0	30.0	21.4
Hf	3.2	4.5	3.9	15.8	11.8	8.4	8.2	4.7
Zr	94	126	96	570	353	290	297	125
Y	4	7	3	46	37	25	52	16
Th	4.9	11.9	1.8	38.0	32.0	26.0	11.7	47.0
U	0.27	2.30	1.21	8.20	5.00	2.80	1.29	2.60
Cu	37	5	10	49	27	24	26	25
Pb	12	37	28	26	31	29	31	28
Zn	65	34	12	85	81	77	82	63
La	20	12	8	115	89	61	83	60
Ce	32	32	7	233	160	118	170	110
Pr	3.4	2.9	1.1	28.0	19.0	14.2	21.0	10.5
Nd	10	10	4	86	61	46	71	31
Sm	1.5	1.9	0.5	13.2	10.9	7.1	13.0	4.4
Eu	0.38	0.41	0.46	1.86	1.74	1.23	1.51	0.61
Gd	1.23	1.57	0.44	10.60	9.00	6.30	11.20	4.00
Tb	0.16	0.24	0.08	1.48	1.26	0.89	1.77	0.51
Dy	0.73	1.26	0.42	8.00	6.80	4.40	9.90	2.80
Ho	0.15	0.23	0.09	1.53	1.34	0.91	1.88	0.62
Er	0.46	0.72	0.30	4.90	3.80	2.60	5.60	1.88
Tm	0.08	0.13	0.05	0.78	0.59	0.40	0.83	0.30
Yb	0.54	0.94	0.48	5.10	3.80	2.70	5.00	1.85
Lu	0.08	0.13	0.11	0.73	0.56	0.40	0.67	0.29
Eu/Eu*	0.82	0.71	2.80	0.47	0.52	0.55	0.37	0.44
$(La/Yb)_n$	25.9	9.5	11.2	16.2	16.8	16.2	11.9	23.3
NK/A	0.75	0.82	0.68	0.81	0.82	0.76	0.90	0.89
A/CNK	1.02	1.09	1.22	0.84	0.82	0.96	1.03	1.05

Rocks: (1–3) gneissose biotite granite; (4–6) quartz monzonite; (7, 8) leucogranite veins hosted in (7) gneissose granite and (8) quartz monzonite. Major components were analyzed by conventional techniques of analytical chemistry at the Geological Institute, Siberian Branch, Russian Academy of Sciences, Ulan-Ude, analysts A.A. Tsyrenova, G.I. Buldaeva, and I.V. Borzhonova; trace elements were determined by ICP-MS on an ELEMENT-2 mass spectrometer at Sobolev Institute of Geology and Mineralogy, Siberian Branch, Russian Academy of Sciences, Novosibirsk. $Eu/Eu^* = Eu_n/(Sm_n \times Gd_n)^{1/2}$; $A/NK = (Na_2O + K_2O)/Al_2O_3$ mol %, $A/CNK = Al_2O_3/(CaO + Na_2O + K_2O)$ mol %. Oxides are given in wt %, and trace elements are in ppm.

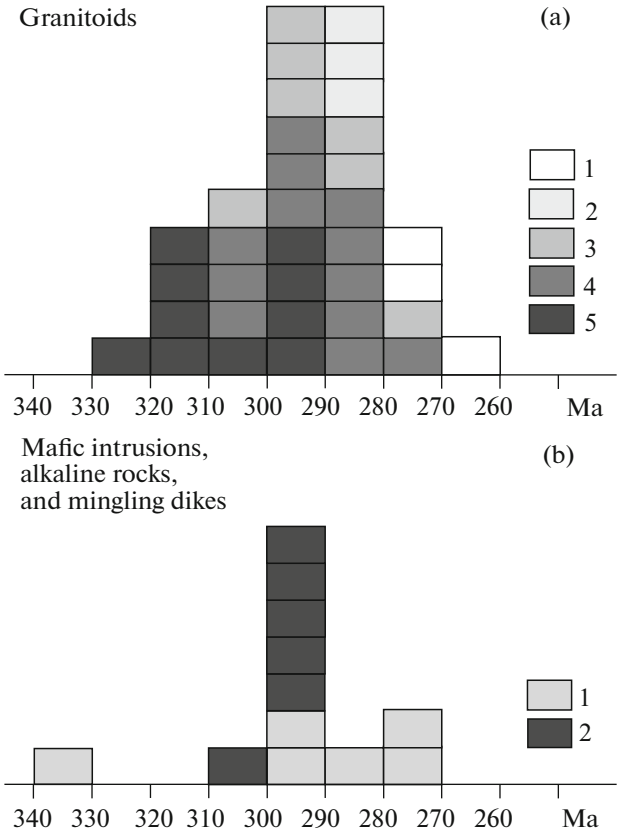

Fig. 3. Histogram showing the distribution of the U–Pb zircon dates of Late Paleozoic magmatic rocks in western Transbaikalia. Granitoid complexes in Fig. 3a: (1) Early Kunalei, (2) Lower Selenga; (3) Zaza; (4) Chivyrkui; (5) Barguzin. Fig. 3b: (1) gabbro–monzonite massifs; (2) alkaline rocks. Based on data from (Yarmolyuk et al., 1997; Tsygankov et al., 2007, 2010, 2012, 2016b; Kovach et al., 2012; Doroshkevich et al., 2012a, 2012b; Khubanov et al., 2016) and data from this publication. If more than one date is available for a massif (dates of discrete intrusive phases), and average age is reported if the dates coincide within the error.

aspect ratio is 2.3–3.5. The crystals are pink, turbid, and host apatite inclusions. The HfO_2 concentrations reach 1.6 wt %. The concordant age (based on $n = 21$ grains) is 305.4 ± 2.9 Ma, MSWD = 1.9 (Fig. 2d). Zircons in the quartz monzonites (sample BG-08) are short-prismatic, 190–210 μm, with an aspect ratio of 1.3–2.5. The crystals are pale pink, transparent, and contain 1.5–2.2 wt % HfO_2. Their concordant age is 291.1 ± 2.5 Ma, $n = 24$, MSWD = 2.7 (Fig. 2f).

A vein of the Zaza-type leucogranite (sample BG-04/3) cutting across the Barguzin gneissose granite (sample BG-4) hosts zircons of two morphological types: (1) pale pink transparent equant short-prismatic crystals (aspect ratio 1.2–1.5) 150–320 μm long, containing up to 1.3 wt % HfO_2, and (2) transparent colorless or pale pink long-prismatic crystals 180–200 μm long very poor in HfO_2 (below the detection limit). We have studied the U–Pb systems of both zircon types and have not detected any significant differences between them. The isotopic age, based on $n = 30$ grains, is 275 ± 1.9 Ma, MSWD = 3.1 (Fig. 2g).

Veins of the Zaza granite (sample BG-07/1) cutting the quartz monzonites (sample BG-07) host dipyramidal zircon crystals whose aspect ratio is 1.3–2.6. The zircons are of bright brown color and practically nontransparent, and their length is no longer than 100 μm. They contain 0.5–1.8 wt % HfO_2. The U–Pb age (based on $n = 21$ grains) is 299.7 ± 2.1 Ma, MSWD = 0.19 (Fig. 2h).

Preexisting literature data and recently obtained isotopic dates are summarized in Fig. 3. These data led us to the following principal conclusions: (1) the dates newly obtained for granitoids of the Barguzin Complex lie within the range of 312–299 Ma, which completely overlaps that age range of 325–290 Ma determined previously for the central part of the granitoid area; (2) the age ranges of granitoids of the Chivyrkui Complex in the eastern Baikal shore and central western Transbaikalia are the same: 305–285 Ma; and (3) the granites of the Zaza Complex are dated at 276 Ma, with this date 10 Ma younger than preexisting dates of these rocks. Note that this unusually young date was obtained on leucogranite from a thin dike cutting the Barguzin gneiss-granite. This dike likely hosts crystalline material produced by the latest portions of the granite melt and, in fact, reflects the lifetime of the deep chambers of the granitoid magmas. Our newly obtained data generally do not show any significant differences in the ages of the granitoids of complexes identified in the central, western, and northern parts of the magmatic area. They also show no any time "zoning" in this area. Both the newly obtained and the preexisting data suggest that the Late Paleozoic magmatic cycle lasted for at least 50 Ma. Another principally important implication is that the mafic and alkaline magmatism occurred simultaneously with the emplacement of the mantle–crustal granitoids. Furthermore, the ages of the Barguzin granites seem to define two maxima at 320–310 and 300–290 Ma, as was previously mentioned in (Tsygankov et al., 2007b). Note that the statistics of the isotopic dates can hardly reflect the volumes of the magmatic products, because each date of the Barguzin granites pertains to an obviously greater rock volume than in other complexes.

The Late Paleozoic (Late Carboniferous to Early Permian) in the Baikal fold area was marked by the origin of a large igneous granite province, which is referred to as the Angara–Vitim batholith (AVB). Note that this term was originally (Salop, 1967) used with reference to the granites of the Barguzin Complex alone, and all other granitoid types were thought to be younger. Obviously, this classification should be revised nowadays, and hence, below we view AVB as composed of all Late Paleozoic granitoids in western

Transbaikalia, except only the alkaline granites and alkali-feldspar syenites of the Early and Late Kunalei complexes. These complexes are excluded in view of the fact that the Mongol–Transbaikalian alkaline granite belt and related volcanic rocks extends far outside the Baikal fold area, whereas AVB granitoids of various type are concentrated within a single area.

GEOCHEMISTRY OF THE LATE PALEOZOIC GRANITOIDS AND RELATED MAFIC ROCKS

Geochemical parameters of Late Paleozoic granitoids in western Transbaikalia are reported in several publications (Reif, 1976; Gordienko, 1987; Litvinovsky et al., 1993; Tsygankov, 2014; Tsygankov et al., 2007b, 2010; Litvinovsky et al., 2002, 2011), and herein we limit ourselves to a brief description of the complexes distinguished previously (Tsygankov et al., 2010) and report the chemical composition of newly collected samples (Table 2) that were used for U–Pb zircon dating.

The granites of the Barguzin Complex, including auto- and allochthonous phases, contain 68–76 wt % SiO_2 and 2.9–6.3 wt % K_2O, which define their affiliation with a high-K calc–alkaline (HK-CA) series (Fig. 4a). The agpaitic index A/NK ≈ 0.7–0.83 (with occasional deviations toward smaller and greater values (up to 0.9 and 0.64, respectively)), and A/CNK ≈ 1 (0.97–1.08). In the classification diagram (Sylvester, 1989), the granites of the Barguzin Complex plot within the field of calc–alkaline high-Al and highly fractionated calc–alkaline (HF-CA) rocks (Tsygankov, 2014). The concentrations of indicator trace elements usually broadly vary (here and below, the concentrations of these elements are given in ppm): Rb (70–240), Sr (150–860), Nb (4–20), and Zr (80–220). In the REE patterns of the HK-CA granites of the Barguzin Complex, LREE strongly dominate over HREE (Fig. 5a): $(La/Yb)_n$ = 18–40. Thereby the autochthonous gneiss-granites are generally depleted in REE compared to the allochthonous types. Most samples show negative Eu anomalies (Eu/Eu* up to 0.45), but some of the porphyritic granites and autochthonous gneiss-granites are not deficient in Eu and, moreover, contain excess Eu, likely due to the presence of residual plagioclase (Fig. 5a).

The average continental crust-normalized patterns of lithophile trace elements (Rudnick and Gao, 2003) display negative Ba, Nb, Ta, P, Eu, and Ti anomalies and positive Th, Pb, Zr, and Hf ones at opposite U behavior (Fig. 6a).

The gneiss-granites sampled for our isotopic geochronologic study are notably different (Table 2, Figs. 4–6). The composition of sample Km-11 is quite typical of the Barguzin Complex, while BG-04 and Km-12 contain more SiO_2, are characterized by low potassic alkalinity, and bear relatively low Rb and REE

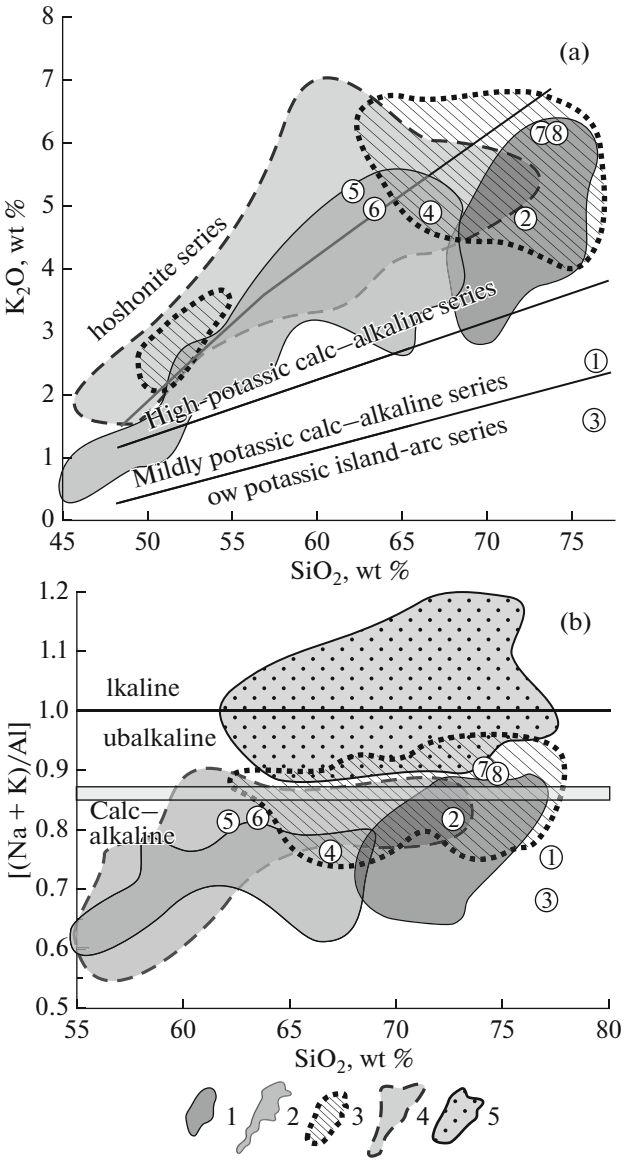

Fig. 4. Classification SiO_2–K_2O and SiO_2–[(Na +K)/ Al] diagrams for Late Paleozoic granitoids in western Transbaikalia. Data are compiled from our original databank on the geochemistry of magmatic rocks from Transbaikalia (Litvinovsky et al., 2011, Supplementary Data). (1) Auto- and allochthonous calc–alkaline granites (Barguzin Complex, 325–290 Ma); (2) high-K calc–alkaline quartz monzonites, quartz syenites, and gabbroids (Chivyrkui Complex, 305–285 Ma); (3) granites and quartz syenites transitional from high-K calc–alkaline to alkaline types with synplutonic mafic rocks (Zaza Complex, 305–285 Ma); (4) high-K monzonite–syenite–quartz syenite intrusive series with synplutonic mafic rocks (Lower Selenga Complex, 285–278 Ma); (5) alkali-feldspar and alkaline granites and syenites of the Mongol–Transbaikalian volcanoplutonic belt (Early Kunalei Complex, 280–273 Ma, and Late Kunalei Complex, 230–210 Ma, not shown in Fig. 4a). Circled numerals show the sampling sites for U–Pb isotopic dating, numerals correspond to sequential numbers in Table 2.

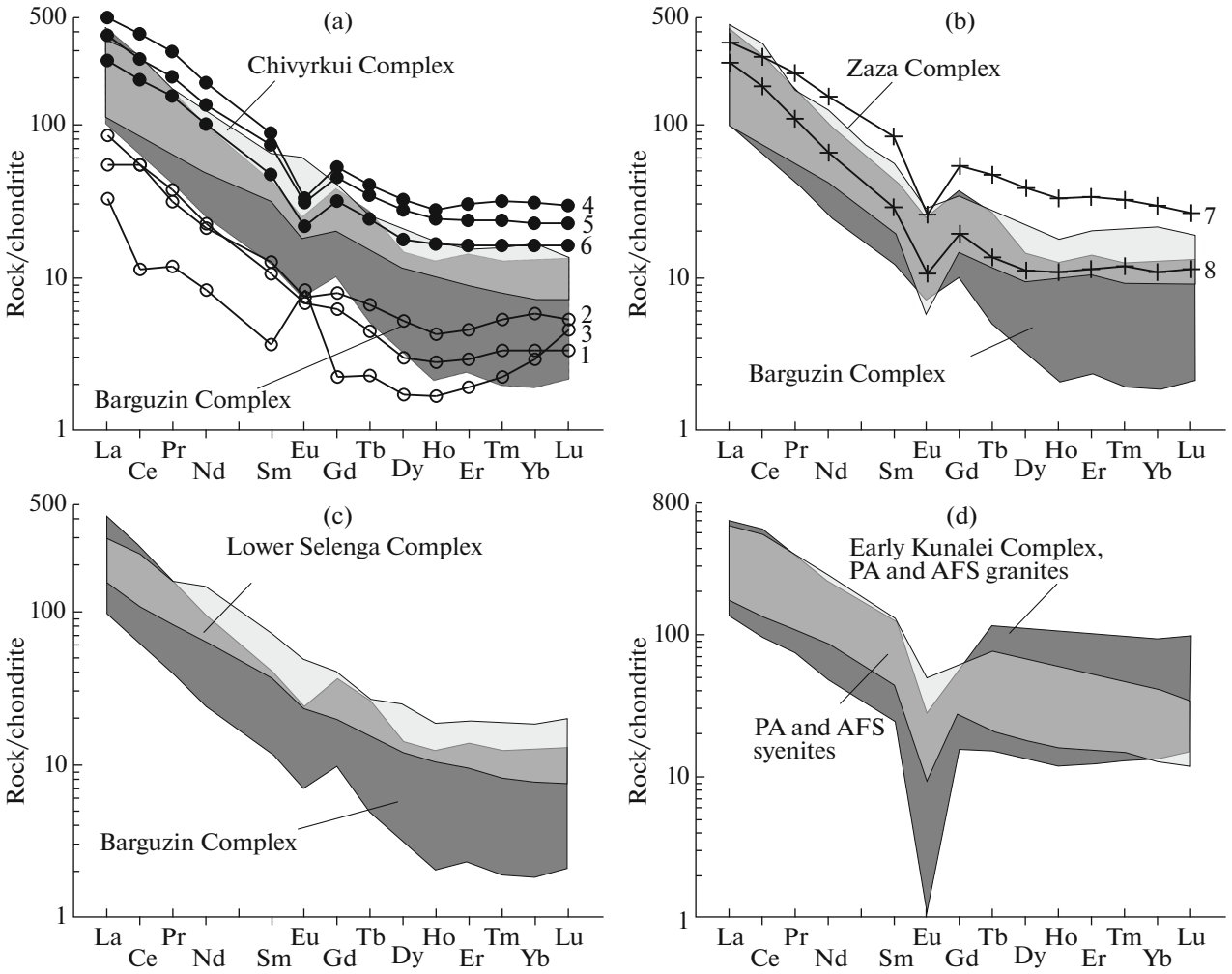

Fig. 5. Chondrite-normalized (Sun and McDonough, 1989). REE patterns of Late Paleozoic granitoids from western Transbaikalia. (a) Calc–alkaline rocks of the Barguzin Complex and high-K calc–alkaline quartz monzonites and quartz syenites of the Chivyrkui Complex; (b) granites and quartz syenites of the Zaza Complex transitional from high-K calc–alkaline to alkaline types; (c) high-K monzonite–syenite–quartz syenite intrusive series (Lower Selenga Complex); (d) Late Paleozoic alkali-feldspar and alkaline granites and syenites of the Early Kunalei Complex. Gray fields show the compositional ranges of the complexes, based on all available samples (our databank on the geochemistry of magmatic rocks from Transbaikalia).

concentrations. The autochthonous gneiss-granites (samples 1–3 in Table 2 and in Figs. 4–6) are noted for the maximum dispersion of the concentrations of major and trace elements, which is likely explained by variations in the segregation of the eutectoid melt and residual material.

The Barguzin granites typically possess negative ε_{Nd} values of −12.8 to −5.2 and a Proterozoic model age of 2.16–1.52 Ga, elevated $\delta^{18}O$ of the zircon and quartz ($\delta^{18}O$ 8.3 – 10.2 and 8.0 – 14.4‰). Considered together with the geological data, isotopic parameters of the rocks definitely indicate that the magmas were derived from a crustal metaterrigenous source.

The calc–alkaline low-Si granites (quartz syenites) of the Chivyrkui Complex, which are rocks transitional from the calc–alkaline and subalkaline types, and the quartz syenites of the Zaza Complex belong, like the Barguzin granites, to a high-K calc–alkaline series (Figs. 4a, 4b). The Chivyrkui Complex consists mostly of quartz syenites and quartz monzonites whose SiO_2 contents are no higher than 69 wt % and whose agpaitic index is <0.8. The A/CNK index increases with increasing silicity of the rocks from 0.71 in the most mafic types to 1.04 in those maximally enriched in silica. Conversely, the Zaza Complex is dominated by highly silicic leucogranites containing up to 77 wt % SiO_2, whereas quartz syenites are subordinate. The agpaitic index A/CNK of the Zaza rocks is not correlated with their silicity and is 0.74–0.96 and 0.89–1.19.

In the classification diagram (Sylvester, 1989), the granites (>68 wt % SiO_2) of the Zaza Complex plot in

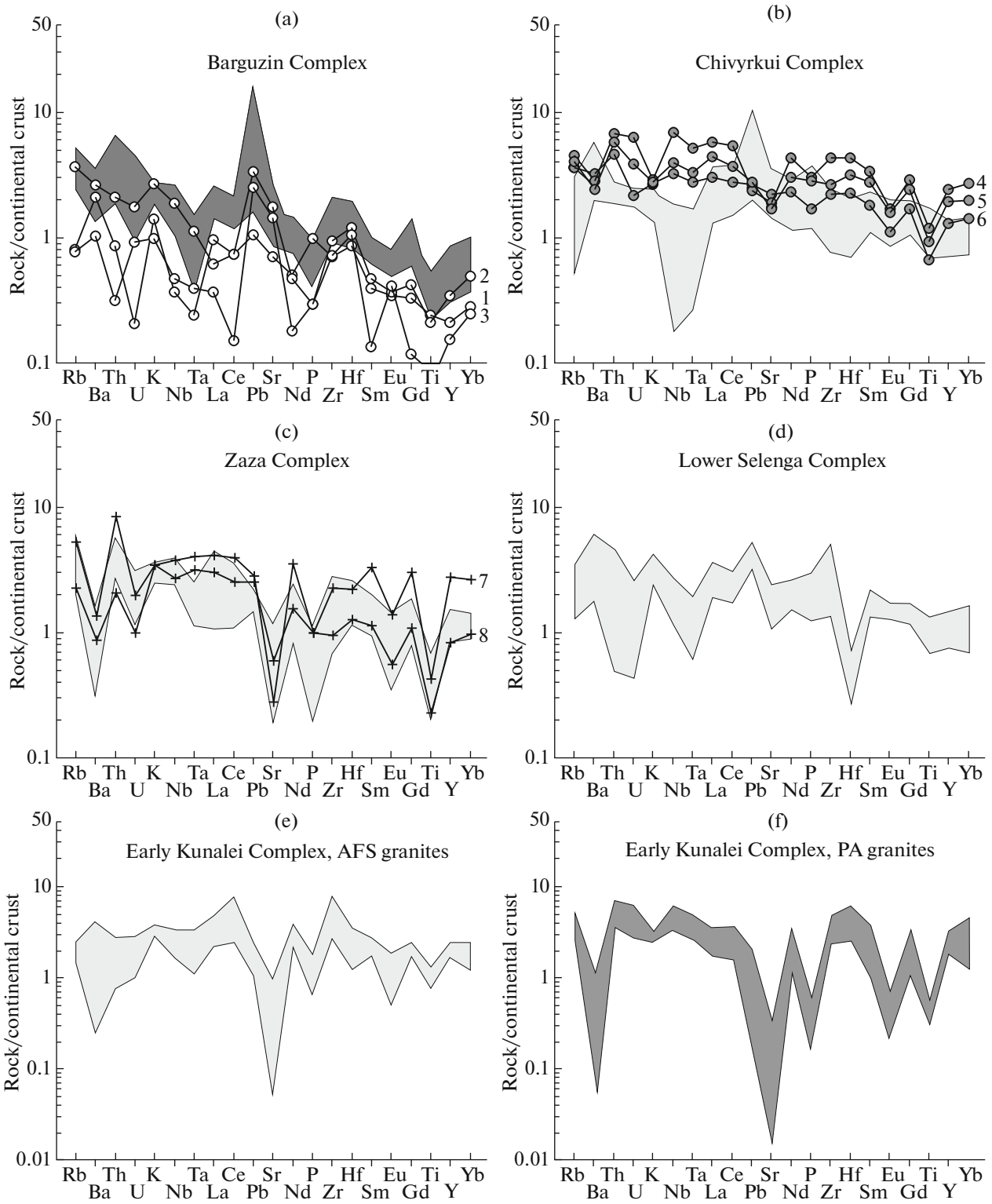

Fig. 6. Continental crust-normalized (Rudnick and Gao, 2003) multielemental patterns for Late Paleozoic granitoids form western Transbaikalia. (a) Calc–alkaline granites of the Barguzin Complex; (b) high-K calc–alkaline quartz monzonites and quartz syenites of the Chivyrkui Complex; (c) granites and quartz syenites of the Zaza Complex, transitional from high-K calc–alkaline to alkaline types; (d) high-K monzonite–syenite–quartz syenite intrusive series (Lower Selenga Complex); (e) Late Paleozoic alkali-feldspar and alkaline granites and syenites of the Early Kunalei Complex.

the field of calc–alkaline and highly fractionated calc–alkaline (HF-CA) rocks (Tsygankov, 2014). Concentrations of trace elements in rocks of the Chivyrkui and Zaza complexes also broadly vary, sometimes as much as by one order of magnitude, and are generally higher than in the Barguzin granites: Rb (25–230 and 57–330), Sr (1220–420 and 670–70), Nb (11–25 and 10–40), and Zr (105–420 and 470–80).

The REE patterns of the rocks of both complexes (Figs. 5a, 5b) are strongly fractionated: $(La/Yb)_n = 9–34$ and 14–34 for rocks of the Chivyrkui Complex and Zaza Complex, respectively. The Zaza granites are characterized by deeper negative Eu anomalies (Eu/Eu* = 0.35–0.57) than the Chivyrkui granites (Eu/Eu* = 0.62–0.75). Some of the rocks do not show a negative Eu anomaly or even display a low positive anomaly (Eu/Eu* = 1.14) owing to feldspar accumulation.

The normalized multielemental patterns best illustrate the differences in the trace-element compositions of the rocks of these complexes (Figs. 6b, 6c). Most samples of the Chivyrkui granitoids do not show any significant anomalies, but some rocks have Ba and Pb and Nb–Ta maxima. Unlike them, the Zaza granitoids typically possess sawtooth-type normalized multielemental patterns, and they are richer in Rb than the Chivyrkui rocks, which is correlated with the elevated potassic alkalinity. The rocks also display Th maxima and are strongly depleted in Sr, P, Eu, Ti, and (not so much) in Ta but do not exhibit Pb maxima (Fig. 6c).

The lately collected geochronologic samples correspond in the classification diagrams (Fig. 4) to rocks of the Chivyrkui and Zaza complexes, but the trace-element composition of these rocks, first of all, the Chivyrkui quartz syenites and quartz monzonites, is noted for slightly higher concentrations of most elements, including REE (Figs. 5a, 6b), and the absence of Nb–Ta minima and Pb maxima in the multielemental patterns. This may be explained by lateral variations in the composition of the rocks of this complex, but information on this issue is still insufficient for any definite conclusions.

The isotopic parameters of the rocks of the Chivyrkui and Zaza complexes are shifted toward the "mantle region" relative to the Barguzin granites (Litvinovsky et al., 2011; Tsygankov, 2014): their ε_{Nd} varies from –10.8 to 0.6, the two-stage model age is 1.97–1.33 Ga, and the oxygen isotopic composition of their zircon and quartz corresponds, respectively, to $\delta^{18}O$ 4.4–7.8 and 8.3–12.2‰. Considered together with geological data (coeval gabbro–monzonite massifs, synplutonic gabbroid intrusions, mingling dikes, and mafic enclaves) and isotopic geochronologic evidence (suggesting that the mafic rocks and granitoids are coeval; Burmakina and Tsygankov, 2013; Tsygankov et al., 2016b), the isotopic parameters testify that the granitoids of these complexes contain a mantle component. The percentage of this component varies from complex to complex, but the material balance indicate that its average contribution is some 25–30% (Tsygankov, 2014).

The Chivyrkui granitoids generally inherit more geochemical characteristics from the precursor Barguzin granites, while the Zaza rocks show certain features of alkaline granitoids that were the youngest rocks of the Late Paleozoic magmatic cycle in Transbaikalia.

The rocks of the Lower Selenga and Early Kunalei complexes are distinguished for the highest total (Early Kunalei rocks) and potassic (Lower Selenga) alkalinity, and the agpaitic index of the monzonites and syenites of the Lower Selenga Complex is commonly no higher than 0.85, which predetermines their calc–alkaline character (Fig. 4). The alkaline granites and alkali feldspathic syenites of the Early Kunalei Complex are typical A-type granites (Whalen et al., 1987, 2006) of the metaluminous (A/CNK<1) alkaline and peralkaline series (Litvinovsky et al., 2002, 2011; Tsygankov, 2014; Tsygankov et al., 2010).

The geochemical parameters of rocks of the Early Kunalei Complex are typical of A-type granitoids: the rocks bear extremely low Sr (Ba) and maximally high Rb, Zr, and Nb concentrations. The Lower Selenga syenites and monzonites are noted for one order of magnitude higher Sr (Ba) concentrations and, correspondingly, lower Nb and Zr concentrations. The REE patterns of syenites and monzonites of the Lower Selenga Complex resemble in several respects those of the Early Kunalei PA granites and AFS syenites (Figs. 5c, 5d, 6d–6f), which also follows from the total REE concentrations and the $(La/Yb)_n$ ratios of 10–27 and 9–24, respectively. The main differences between the REE patterns are the different "depths" of the Eu anomalies, which is poorly pronounced (if any) in the rocks of the Lower Selenga Complex (Eu/Eu* = 0.59–1.0) but reaches a maximum (Eu/Eu* up to 0.14) in the AFS syenites and, particularly, PA granites of the Early Kunalei Complex. The normalized multielemental patterns of rocks of similar silicity (syenites and monzonites) of the Lower Selenga and Early Kunalei complexes reflect differences between the calc–alkaline and alkaline (A-type granitoids) series. The latter are characterized by deep negative Ba, Sr, P, Eu, and Ti anomalies, whereas rocks of the calc–alkaline series are depleted in Nb, Ta, and Hf and are sometimes enriched in Pb.

The isotopic parameters of the rocks of the Lower Selenga Complex are closely similar to those of the granitoids of the Chivyrkui and Zaza complexes (Tsygankov, 2014), which also suggests a mixed mantle–crustal source of the magmas. In the alkaline granites and alkali feldspar syenites of the Early Kunalei Complex, ε_{Nd} is negative and close to zero (from –4.1 to –0.1), and $\delta^{18}O$ of the quartz is 8.5–6.4. With regard for the empirical value of $\Delta\ \delta^{18}O_{Qtz\text{-}Zrn} =$

3.1–3.5‰ Tsygankov, 2014), it is reasonable to believe that the partial melt of the alkaline granitoids was derived from a juvenile mantle source with $\delta^{18}O = 5.3 \pm 0.3$‰ (Valley et al., 1998).

Each of the intrusive complexes described above, except only the Barguzin Complex, is associated with mafic rocks (basaltic andesites and trachybasaltic andesites), which are found as small gabbro–monzonite plutons, synplutonic intrusions, mingling dikes, and mafic enclaves (Tsygankov et al., 2016b). Although these rocks occur in the form of broadly diverse geological bodies, their chemical composition varies relatively little, regardless of the affiliation of the rocks with certain complexes (Tsygankov et al., 2010, 2016b; Litvinovsky et al., 2011). These are low-Mg trachybasalts and trachybasaltic andesites, Mg# = 100 × (MgO/(MgO + FeO*), mol % = 52–40, with relatively little TiO_2 (0.8–1.5 wt %), except only for the mafic rocks in association with the granitoids of the Lower Selenga Complex (which contain up to 2.4 wt % TiO_2) and relatively much Al_2O_3 (15–20 wt %), and high potassic alkalinity (Tsygankov et al., 2016b).

The rocks are enriched in LREE relative to HREE, $(La/Yb)_n = 8–23$, and their Eu anomalies (either negative or positive) are poorly pronounced or are not pronounced at all (Eu/Eu* 0.67–1.25). The OIB-normalized patterns of lithophile elements of mafic rocks related to the Late Paleozoic granitoids in Transbaikalia show the same (or closely similar) geochemical signatures, which likely reflect similarities between the magmatic sources: these are the strong depletion in Nb (and not as strong in Ti, Zr, and Hf), enrichment in LILE, and positive Pb and Sr anomalies.

The general evolution of Late Paleozoic magmatism in Transbaikalia thus shows an increase in the alkalinity of the successively produced intrusive complexes (Litvinovsky et al., 2011; Tsygankov et al., 2010; Tsygankov, 2014) at merely insignificant variations in the composition of the related mafic rocks. This general evolutionary trend is complicated by the simultaneous origin of various granitoid complexes (Chivyrkui–Zaza, partly Barguzin, and Lower Selenga–Early Kunalei), which differ from one another in the rocks and in their geochemical specifics. These compositional variations are associated with a decrease in the amount of the products of magmatism with time.

GEODYNAMICS OF BATHOLITH-FORMING PROCESSES

The geodynamic environment of Late Paleozoic magmatism in western Transbaikalia is a matter of long-lasting and hot discussions, which are mostly centered around the following models: a plume model (Yarmolyuk et al., 1997, 2013, 2014, 2016), a model of an active continental margin (Rytsk et al., 1998; Zorin, 1999; Donskaya et al., 2013), a postcollisional model (Tsygankov et al., 2010; Litvinovsky et al., 2011), and a model of delamination of the crust of a collisional orogen (Gordienko et al., 2003; Kiselev et al., 2004). The diversity of the viewpoints results from the various paradigms and differences in interpretations of available information. This uncertainty stems first and foremost from the scarcity of geological data on processes that took place immediately before the massive formation of the granites. This is explained primarily by the fact that the pre-granite rocks are preserved only fragmentarily in the form of separated relict fragments of various size. The geodynamic nature of the tectono–stratigraphic complexes composing these fragments is often disputable, and it is hard to correlate them with analogous rocks found in nearby areas because of the paucity of the geological information. Nevertheless geological and geochronologic data obtained over the past two decades make it possible to formulate certain boundary conditions that should be taken into account when the Late Paleozoic geodynamics of the area is analyzed.

The Angara–Vitim batholith was produced in the Late Paleozoic (in the Late Carboniferous to Early Permian) at approximately 325 to 270 Ma. The intensity of granite-forming processes at that time likely varied, although these variations have not still been quantified. As was mentioned above, the statistics of the isotopic dates cannot be regarded as adequately reflecting the actual variations in the intensity of magmatism of certain type in view of the significant differences between the granitoids forming AVB.

Considered together, geological, isotopic geochronologic, and geochemical data suggest that magmatism in this area evolved from typical crustal (Barguzin type) to mixed mantle–crustal (all other complexes in AVB), with a gradual systematic increase in the content of the mantle component in the magmatic source (Tsygankov et al., 2010; Tsygankov, 2014; Litvinovsky et al., 2011). A mantle constituent is ubiquitously discernable, for example, in the form of associated mafic and alkaline magmatism, only in the post-Barguzin granitoids (Tsygankov et al., 2016b; Doroshkevich et al., 2012a, 2012b). In other words, the Barguzin granites are, geologically, the oldest in the region, in spite of the significant overlap of the isotopic geochronologic dates (Fig. 3).

In the Late Devonian–Early Carboniferous, the area currently occupied by the Baikal fold area was a relatively shallow-water marine basin with terrigenous–carbonate sedimentation. The geodynamic nature of this basin is not fully understood and so far disputable: whether it was a foreland-type basin (Filimonov et al., 1999), a pull-apart basin, or a passive continental margin (Ruzhentsev et al., 2012; Minina, 2014). No later than the mid-Carboniferous, the sediments accumulated in the basin were intensely deformed (Hercynian orogeny). The extent and scale of folding and thrusting during that time and the driving geodynamic forces of these processes are disput-

able. For example, several researchers are prone to believe that the granitoids were derived in a thickened (even doubled) crust (Litvinovsky, 1993; Gordienko, 2003), but no data in support of this hypothesis has been collected as of yet.

With regard for the aforementioned constraints, below we analyze the model of the Late Paleozoic geodynamics of Transbaikalia in the context of the origin of AVB.

The model of a Late Paleozoic continental margin is favored by quite numerous geologists (Rytsk et al., 1998; Zorin, 1999; Donskaya et al., 2013). These hypotheses are underlain by both general schemes of the geodynamic evolution of the area and geochemical data, first of all, so-called "subduction signatures": negative Nb–Ta anomalies in the normalized trace-element patterns of the granitoids and related mafic rocks and negative ε_{Nd} values.

The opponents of these ideas put forth the following arguments. Late Paleozoic magmatism in Transbaikalia generally occurred at significant territories, but not within linear zones, as is the case with such typical active continental margins as the modern South American Andes or Cretaceous Okhotsk–Chukotka volcano-plutonic belt. For example, the widely known Coastal Batholith in Peru trends for 1600 km, at a width of approximately 65 km, parallel to the strike of the Peru–Chile deep sea trench (*Magmaticheskie...*, 1985). Similar morphologies are also typical of other large granitoid batholiths in active continental margins but is absolutely atypical of western Transbaikalia. The plutonic rocks of AVB are dominated by granodiorites, tonalites, and plagiogranites, which are absent from (tonalites and plagiogranites) or are scarce (granodiorites) among the Late Paleozoic granitoids of Transbaikalia. Moreover, no volcanic rocks of andesitic (widely speaking) composition of this age have ever been found in Transbaikalia, whereas Cambrian carbonate Devonian–Early Carboniferous terrigenous rocks are locally preserved, and this suggests that the erosion depth is relatively shallow. Subduction-related geochemical signatures were identified in mafic rocks in Transbaikalia until the latest Cretaceous, i.e., until the time when no subduction beneath the southern margin (in modern coordinates) of the North Asian continent can be inferred from any data. Moreover, such geochemical signatures (negative Ta–Nb anomalies) themselves are not an unambiguous indicator of subduction-related magmatism (Farmer, 2003).

The models of delamination of the crustal base of lithospheric mantle in a collisional orogen seem to be more realistic (Gordienko et al., 2003; Kiselev et al., 2004). Delamination is understood in this context as the breakaway of the lower levels of the thickened eclogitized crust and upper mantle and their fast subsidence into the asthenosphere (Bird et al., 1979; Houseman et al., 1981). The hot low-density asthenospheric mantle substitutes thereby the separated portion of the denser (eclogites) lithosphere, and this is associated with the rise of the geoisotherms and the derivation of basaltic magmas, which in turn, facilitate the melting of the orogen. This model is devoid of most of the aforementioned inconsistencies and was validated by model simulations (Kiselev et al., 2004), which testify that this mechanism is principally possible. According to (Gordienko et al., 2003), large-scale poscollisional granite-forming processes in Transbaikalia in the Carboniferous–Permian were induced by crustal overthickening in the Ordovician–Silurian and Devonian collision. A key role in this model is played by the timing and extent of the collisional processes before the origin of AVB. Thereby one should take into account that the consolidation of the heterogeneous basement of the Baikal fold area likely terminated no later than in the Ordovician–Silurian as a consequence of the accretion of the Uda–Vitim and Dzhida island arcs and the docking of the Tuva–Mongolian microcontinent to the southern (in modern coordinates) margin of Siberia (Gordienko et al., 2007, 2010; Bulgatov and Gordienko, 1999). In other words, the pre-granite basement of the Baikal fold area was produced at least 100 Ma before the onset of massive derivation of the granites.

A new episode of folding and metamorphism began in the mid-Carboniferous, as follows from the deformations of the Late Devonian–Early Carboniferous rocks (Ryzhentsev et al., 2012). The geological relations and isotopic age of the Barguzin granites (Tsygankov et al., 2010) indicate that the processes producing them started late during the Hercynian orogeny. A pivoting problem therein is the extent of this orogeny. It is uncertain whether the crust was indeed significantly thickened, as is necessary for delamination. No direct evidence is recovered so far to solve these problems, but the following circumstantial considerations can and should be taken into account. For instance, the occurrence of large (100 km^2 and larger) relict fragments of the practically unmetamorphosed Early Paleozoic volcanic and carbonate rocks suggests that the erosion depth could hardly exceed 10 km. These considerations are consistent with data reported in (Reif, 1976). According to these estimates, the Barguzin granites crystallized at a depth of 8–12 km. At a modern thickness of the crust in the Baikal fold area of approximately 40 km (Suvorov et al., 2002), the crust thickness of the Hercynian orogen during the onset of the granite-forming processes was no less than 55–60 km. At the same time, delamination becomes possible (Gordienko et al., 2003 and references therein) at a crustal thickness of at least 50 km, i.e., just a little bit lower than the aforementioned estimates. It seems to be hardly possible in these circumstances that an eclogite layer thick enough to be prone to delamination could be formed. The Hercynian orogenic processes were likely local and could not result in any significant thickening of the crust of the Baikal fold area, and this constrains the applica-

bility of the delamination model to explaining the origin of AVB.

The Hercynian orogeny in the southern folded surroundings of the Siberian craton is a starting point for the "postcollisional model" of Late Paleozoic magmatism in this area. According to (Liégeois et al., 1998; Bonin, 2004), the postcollisional period of time began after the termination of collision of two or more "continental" plates and associated high-temperature metamorphism. Postcollisional magmatism is constrained to areas within continents that are characterized by still continuing significant horizontal motions of the terranes along mega-shear zones. These motions immediately predate the transition to a typical intraplate regime, with the dominance of extension, and to continental rifting. One of the principally important characteristics of postcollisional magmatism is the wide occurrence of high-K calc–alkaline granitoids (Zhao et al., 2008; Whalen et al., 2006), i.e., exactly what granitoids of the Angara–Vitim batholith are (Tsygankov et al., 2010). It is thought that massive crustal melting is triggered by the emplacement of mafic magmas, which were reportedly generated due to the decompressional melting of an upper mantle source (Tsygankov et al., 2010, 2016b; Tsygankov, 2014; Litvinovsky et al., 2011). The origin of the alkaline granitoids marks the transition to an intraplate (rift) evolutionary episode.

The soft spot of this model is the absence of mega-shear zones (at least they have not been found so far) and related near-shear extensional structures (for example, pull-apart basins) to which the decompressional melting of the mantle could be related as a condition necessary for large-scale crustal granite-forming processes. We cannot rule out that these structures were "healed" by the granitoids and are thus indiscernible, but the postcollisional model remains vulnerable until evidence of such structures are found.

The plume model of Late Paleozoic and Early Mesozoic batholith-forming processes in Central Asia is discussed in several publications (Yarmolyuk et al., 1997, 2013, 2014, 2016) and is devoid of the aforementioned inconsistencies. At the same time, this model introduces a certain element of contingency into the geological evolutionary history of Siberia. For example, it is worth mentioning the complicated loop-shaped movement trajectory of Siberia (Yarmolyuk et al., 2013, 2016) with the discrete episodes responsible for the origin of giant batholiths: Angara–Vitim (300 Ma), Khangai (250 Ma), and Khentei (210 Ma). Thereby the Khangai batholith was produced practically simultaneously with the Siberian flood basalts, and AVB was largely synchronized with the Tarim plume (Dobretsov et al., 2010; Xu et al., 2014; Yarmolyuk et al., 2014). The cause-and-effect relations between the flood-basalt and granitoid magmatism are still obscure, as also are the factors that controlled the compositionally contrasting character of plume magmatism (flood basalts and granitoid batholiths). Furthermore, the duration of the processes that produced AVB is several times longer than the duration of the largest scale plume-related magmatic processes, such as those that produced, for example, the Siberian flood basalts (Reichow et al., 2009).

DISCUSSION

The above review shows that a pivoting role in all of the models is assigned to mafic magmas, whose coevalness with the granite-forming processes follows from geological relations and isotopic geochronologic data. These puts forth the problem of the possible differences between mafic magmas of plume origin and those produced in relation to subduction, delamination, and/or decompression. Geological manifestations of mafic magmatism related to Late Paleozoic granitoids in western Transbaikalia can hardly clarify this issue, and hence, the only criterion of the geodynamic nature of the mafic magmas is their geochemical parameters: a trachybasalt or trachybasaltic andesite composition, low Mg#, relatively low TiO_2 content, elevated Al#, and relatively high to high alkalinity. All of the mafic rocks are typically enriched in LREE relative to HREE, show poorly pronounced Eu anomalies (if any), negative Ta and Nb anomalies (and to a lesser extent, also Ti, Zr, and Hf anomalies), high LILE concentrations, positive Pb and Sr anomalies, and negative ε_{Nd} values (Tsygankov et al., 2010, 2016b; Litvinovsky et al., 2011).

Analysis of the canonical ratios of highly incompatible elements characterizing the composition of the magmatic sources (Kovalenko et al., 2009) and the isotopic composition of the mafic rocks suggests that their melts were derived from phlogopite- and garnet-bearing lherzolite lithospheric mantle that was enriched in a crustal component, which was melted in a "hydrated" environment (phlogopite decomposition) at a pressure of 25 kbar and temperature >1000°C (Tsygankov et al., 2016b). Mafic magma derivation in hydrated environments is usually thought to occur in subduction zones, but other scenarios are also possible, for example, the reactivation of a subduction-modified (metasomatized) mantle source (Puffer, 2003) under the effect of a mantle plume. Support for this hypothesis is provided by similarities between the Early Paleozoic island-arc (Tsygankov et al., 2016a) and Late Paleozoic intraplate (Tsygankov et al., 2016b) mafic rocks whose melts were derived from sources enriched in crustal material. It can be hypothesized that this enrichment could have taken place in the Early Paleozoic during the subductional episode (Uda–Eravna–Dzhida island arc) in the geological evolution of the region (Gordienko, 2006; Gordienko et al., 2007, 2010; Tsygankov et al., 2016b). Moreover, the geochemical characteristics of the Late Paleozoic mafic rocks are strikingly similar to the average composition of low-Ti basalts in the Sibe-

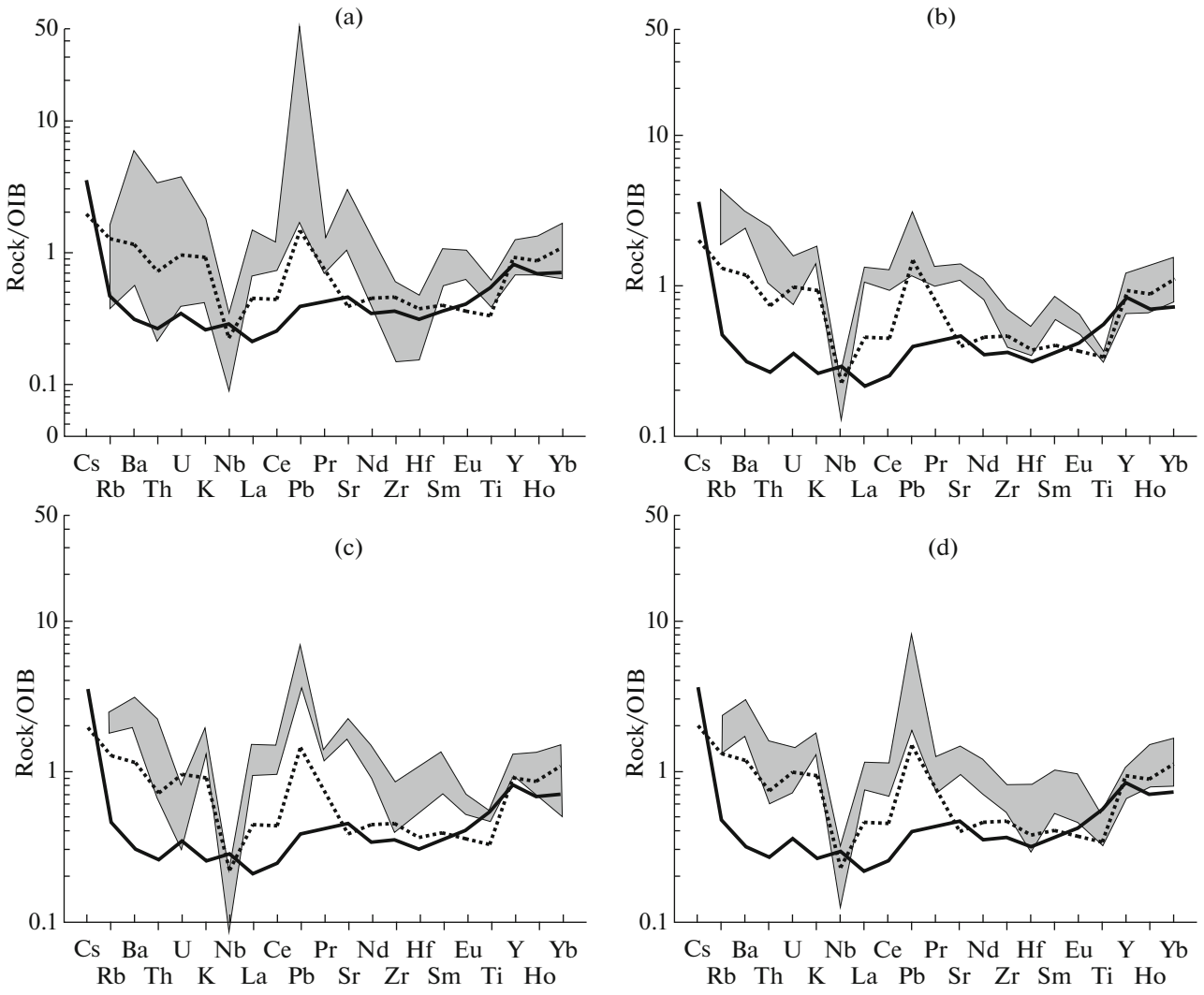

Fig. 7. OIB-normalized (Sun and McDonough, 1989) multielemental patterns for mafic rocks related to Late Paleozoic granitoids in western Transbaikalia. (a) Gabbroids of the Chivyrkui Complex; (b) mafic constituent in mingling dikes and synplutonic amphibole gabbro of the Zaza Complex; (c) mafic rocks in mingling dikes of the Lower Selenga Complex; (d) trachybasalts related to alkaline granitoids of the Early Kunalei Complex. Solid line corresponds to high-Ti basalts, and dotted lines show low-Ti basalts among Siberian flood basalts (Farmer, 2003).

rian flood-basalt province (Fig. 7), whose intraplate nature leaves no much doubt (Farmer, 2003). This means that hydrated melting conditions of the metasomatized mantle can occur not only in subduction zones but also in intraplate geodynamic environments.

An important argument in support of the intraplate nature of Late Paleozoic magmatism in Transbaikalia is provided by ijolite–urtite, nepheline and alkali-feldspar syenite intrusions that are constrained within two stripes of northeastern strike: the Synnyr and Saizhen complexes. The U–Pb zircon age of the alkaline rocks from a number of closely spaced massifs in the Vitim Highland is 520–486 and 303–293 Ma (Doroshevich et al., 2012a, 2012b), and the Sr and Nd isotopic composition of the rocks of various age is practically the same (Doroshkevich et al., 2012). Hence, first, the alkaline magmatism shows certain inherited features, and this resembles the relations between Early and Late Paleozoic mafic rocks in this area, and second, the mafic rocks were obviously formed simultaneously with the extensive granite-forming processes.

Finally, it is pertinent to stress the setting of the Mongol–Transbaikalian volcano-plutonic belt, whose hundreds of massifs occur within the outlines of the Angara–Vitim batholith, and the belt itself is traced far beyond it (Litvinovsky et al., 2002; Jahn, 2004; Jahn et al., 2009). The alkaline granitoids and related volcanic rocks of this belt were produced at 280–220 Ma (Litvinovsky et al., 2002; Reichow et al., 2010). The

alkaline granites and alkali-feldspar syenites are of type A and are often associated with volcanic rocks of trachybasalt–trachyrhyolite and comendite composition, as is typical of intraplate environments.

The available geological, geochemical, and isotopic geochronologic data are generally consistent with the intraplate–plume nature of the Late Paleozoic granitoid and simultaneous mafic and alkaline magmatism in western Transbaikalia. At the same time, it is pertinent to recall the fact that the alkaline and mafic rocks (whatever their modes and forms of occurrence) were found only in the post-Barguzin granitoids. Their total volume is much smaller (likely no more than a few percent) than that of the granitoids. AVB is dominated by granites of the Barguzin Complex, which make up no less than two-thirds of all Late Paleozoic magmatic rocks in the area. The Barguzin granitoids typically compose autochthonous facies, host relics and fragments of metamorphic rocks, possess low negative ε_{Nd} values of -10 to -14, have model ages of 1.5 to 2.0 Ga, are characterized by high $I_{Sr} > 0.707$, and show elevated $\delta^{18}O = 14–10‰$ of their quartz and zircon. These parameters point to a crustal nature of the granitoid magmas, which should have been derived via melting metaterrigenous protoliths without any appreciable addition of juvenile material.

This means that we shall explain, within the framework of the plume model, the insignificant volume of the mafic rocks and the dominance of the granites by their types produced by melting crustal metaterrigenous protoliths. Thereby the following considerations should be taken into account. Judging from the marginal portions of the autochthonous granite massifs (venite and stromatite migmatites) and the composition of xenoliths (crystalline schists) in the allochthonous granites, the magmas of the Barguzin granitoids were derived at depths no greater that 20–25 km, i.e., under pressures of about 6–8 kbar (no more accurate estimates are available so far). The temperature at this depth should have been 600–700°C (at an "orogenic" geothermal gradient), and the metamorphic rocks should have contained no more that 1–2% fluid (in micas and amphiboles). We assume that the average thickness of the "layer" of the Barguzin granites was 8 km (including the eroded rocks). The crust of a collisional orogen at a depth of 20–25 km was of intermediate composition, and the degree of its melting may have been 50–60%. With regard for these constraints, a granite "layer" of the aforementioned thickness can be produced by remelting a layer of crustal material no less than 15 km thick, and not in the base of the crust, as it is usually assumed, but in its intermediate, cooler portion.

Assuming that the mafic magmas served as that same additional heat source that induced extensive melting, and taking into considerations model simulations in (Huppert and Sparks, 1988), we arrive at the conclusion that the basaltic magma "layer" able to induce this melting should have been at least twice as thick as the granite "layer", i.e., no thinner than 15 km. Ascending to the surface, the basaltic magmas should have pooled in the middle crust, but not in its base, as follows from underplating models (Bryan et al., 2010), or even at the uppermost levels, as is the case with several areas of plume magmatism worldwide. These oversimplified considerations show that granite melts able to produce a rock volume equal to the Angara–Vitim batholith can be derived under the effect of a comparable volume of basaltic magmas in the middle crust. In this context it should be mentioned that no large anomalies have ever been detected in the density structure of the crust of the Baikal fold area (Suvorov et al., 2002). This means that no evidence of mafic magmas that could induce massive crustal melting has ever been found. This also pertains to all models that were discussed above and that assign a key role to mafic mantle magmatism.

More than two decades ago, Litvinovsky and his coauthors (Litvinovsky et al., 1993) suggested a model of crustal melting in an open water-saturated system, with water coming from a mantle diapir. Obviously, water brought into a magma-generation region should have significantly facilitate the melting process, but nevertheless the above reasoning pertaining to the volume relations (strongly underestimated amounts of the basaltic magmas) are valid with regard for the volume of aqueous fluid that could potentially be separated from crystallizing basaltic melt.

With regard for the realistic assumption of an intraplate geodynamic environment in which the Angara–Vitim batholith should have been formed, it should be admitted that the only driving force of the extensive granite-forming processes could be a mantle plume. At the same time, the absence of any discernible density anomalies underlying the granite "layer" suggests that the mechanisms of the lithosphere–plume interaction were likely more complicated than the simple melting of crustal protoliths due to the conduction-controlled heat transfer from mafic intrusions.

CONCLUSIONS

Our newly obtained isotopic geochronologic data on the northwestern part of the Angara–Vitim granitoid batholith are consistent with our earlier estimates (Tsygankov et al., 2010) of overall duration of the Late Paleozoic magmatic cycle at no less than 55 Ma (from 325 to 280 Ma). These data also indicate that the onset of alkaline mafic magmatism in western Transbaikalia was synchronous with the transition from crustal granite-forming processes to the origin of granitoids of mixed mantle–crustal type, with a gradual increase in the percentage of juvenile material in the magmatic source.

Analysis of the geodynamic models currently adopted for the regional Late Paleozoic magmatism shows that a key role in all of them is assigned to massive granite derivation under the effect of mafic magmas in various assumed geotectonic regimes: subduction, delamination, decompression, and a mantle plume. The plume model is best consistent with the intraplate nature of AVB. At the same time, one should be aware that the derivation of a vast volume of the granitoids (about 1 million km^3) should have required a comparable volume of mafic magmas localized at mid-crustal levels in the Baikal fold area, which still has not found supporting evidence in the density structure of the regional crust. Its means that the mechanism of plume–lithospheric interaction that induced extensive crustal melting and the origin of the vast granitoid areas was more complicated than the simple heat conduction-controlled melting of crustal protoliths in contact with mafic intrusions.

ACKNOWLEDGMENTS

The authors thank the reviewers A.A. Nosova and A.V. Chugaev (IGEM RAS) for constructive criticism that led us to improve the manuscript. This study was financially supported by Grant 15-17-10010 from the Russian Scientific Foundation (principal investigator A.A. Tsugankov) and the Russian Foundation for Basic Research (Siberia), project no. 15-45-04208 (principal investigator G.N. Burmakina).

REFERENCES

Belichenko V.G., Geletii N.K., and Barash I.G., Barguzin microcontinent (Baikal mountain are): the problem of outlining, *Russ. Geol. Geophys.,* 2006, vol. 47, no. 10, pp. 1035–1045.

Bird, P., Continental delamination and the Colorado plateau, *J. Geophys. Res.,* 1979, vol. 84, pp. 7561–7571.

Bonin, B., Do coeval mafic and felsic magmas in post-collisional to within-plate regimes necessarily imply two contrasting, mantle and crustal, sources? A review, *Lithos,* 2004, vol. 78, pp. 1–24.

Bryan, S.E., Peate, I.U., Peate, D.W., et al., The largest volcanic eruptions on Earth, *Earth Sci. Rev.,* 2010, vol. 102, pp. 207–229.

Bulgatov, A.N. and Gordienko, I.V., Terrains of the Baikal mountain range and the location of gold deposits, *Geol. Ore Deposits,* 1999, vol. 41, no. 3, pp. 204–213.

Burmakina, G.N. and Tsygankov, A.A., Mafic microgranular enclaves in Late Paleozoic granitoids in the Burgasy quartz syenite massif, western Transbaikalia: composition and petrogenesis, *Petrology* 2013, vol. 21, no. 3, pp. 280–303.

Dobretsov, N.L., Borisenko, A.S., Izokh, A.E., and Zhmodik, S.M., A thermochemical model of Eurasian Permo–Triassic mantle plumes as a basis for prediction and exploration for Cu–Ni–PGE and rare-metal ore deposits, *Russ. Geol. Geophys.,* 2010, vol. 51, no. 9, pp. 903–924.

Donskaya, T.V., Gladkochub, D.P., Mazukabzov, A.M., and Ivanov, A.V., Late Paleozoic–Mesozoic subduction-related magmatism at the southern margin of the Siberian continent and the 150 million-year history of the Mongol–Okhotsk ocean, *J. Asian Earth Sci.,* 2013, vol. 62, pp. 79–97.

Doroshkevich, A.G., Ripp, G.S., and Sergeev, S.A., U–Pb (SHRIMP-II) isotope dating of zircons from alkali rocks of Vitim Province, West Transbaikalia, *Dokl. Earth Sci.,* 2012a, vol. 443, no. 1, pp. 297–301.

Doroshkevich A.G., Ripp G.S., Sergeev S.A., and Konopel'ko D.L., The U–Pb geochronology of the Mukhal alkaline massif (western Transbaikalia), *Russ. Geol. Geophys.,* 2012b, vol. 53, no. 2, pp. 169–174.

Doroshkevich, A.G., Ripp, G.S., Isbrodin, I.A., and Savatenkov, V.M., Alkaline magmatism of the Vitim Province, West Transbaikalia, Russia: age, mineralogical, geochemical and isotope (O, C, D, Sr and Nd) data, *Lithos,* 2012, vol. 152, pp. 157–172.

Farmer, G.L., Continental basaltic rocks, in *Treatise on Geochemistry,* Amsterdam: Elsevier, 2003, vol. 3, pp. 85–121.

Filimonov, A.V., Minina, O.R., and Neberekutina, L.N., Urmin sequence as the reference Upper Devonian stratotone of West Transbaikalia, Vestn. Voronezhsk. Gos. Univ., Ser. Geol., 1999, no. 8, pp. 46–57.

Gordienko, I.V., *Paleozoiskii magmatizm i geodinamika Tsentral'no-Aziatskogo skladchatogo poyasa* (Paleozoic Magmatism and Geodynamics of the Central Asian Foldbelt), Moscow: Nauka, 1987.

Gordienko, I.V., Geodynamic evolution of Late Baikalides and Paleozoids in the folded periphery of the Siberian Craton, *Russ. Geol. Geophys.,* 2006, vol. 47, no. 1, pp. 51–67.

Gordienko, I.V., Kiselev, A.I., and Lashkevich, V.V., Delamination lithosphere and related magmatism in folded areas: evidence from folded framing of the southern Siberian Platform, in *Problemy global'noi geodinamiki: Materialy teoreticheskogo seminara OGGGGN RAN* (Problems of Global Geodynamics: Proceedings of Theoretical Seminar of OGGGGN RAN), Rundkvist, D.V., Ed., Moscow: GEOS, 2003, pp. 185–199.

Gordienko, I.V., Filimonov, A.V., Minina, O.R., et al., Dzhida island-arc system in the Paleoasian ocean: structure and main stages of Vendian–Paleozoic geodynamic evolution, *Russ. Geol Geophys.,* 2007, vol. 48, no. 1, 91–106.

Gordienko, I.V., Bulgatov, A.N., Ruzhentsev, S.V., et al., The Late Riphean–Paleozoic history of the Uda–Vitim island-arc system in the Transbaikalian sector of the Paleoasian ocean, *Russ. Geol Geophys.,* 2010, vol. 51, no. 5, pp. 589–614.

Houseman, J.A., McKenzie, D.P., and Molnar, P., Convective instability of a thickened boundary layer and its relevance for the thermal evolution of continental convergent belts, *J. Geophys. Res.,* 1981, vol. 86, pp. 6115–6132.

Huppert, H.E. and Sparcks, R.S.J., The generation of granitic magmas by intrusion of basalt into continental crust, *J. Petrol.,* 1988, vol. 29, pp. 596–624.

Jahn, B.M., The Central Asian orogenic belt and growth of the continental crust in the Phanerozoic, *Geol. Soc. London, Sp. Publ.,* 2004, vol. 226, pp. 73–100.

Jahn, B.M., Litvinovsky, B.A., Zanvilevich, A.N., and Reichow, M.K., Peralkaline granitoid magmatism in the Mongolian-Transbaikalian belt: evolution, petrogenesis

and tectonic significance, *Lithos,* 2009, vol. 113, pp. 521–539.

Karta magmaticheskikh formatsii yuga Sibiri i Severnoi Mongolii. Masshtab 1 : 1500000 (1 : 1500000 Map of Magmatic Formations of Southern Siberia and North Mongolia), Moscow: MinGeo, 1989.

Khubanov, V.B., Bimodal Dike Belt of Central Part of West Transbaikalia: geological Structure, Age, Composition, and Genesis, *Extended Abstract of Candidate (Geol-Min.) Sci.,* Ulan-Ude: GIN SO RAN, 2009. 23 s.

Khubanov, V.B., Buyantuev, M.D., and Tsygankov, A.A., U–Pb dating of zircons from PZ_3–MZ igneous complexes of Transbaikala by sector-field mass spectrometry with laser sampling: technique and comparison with SHRIMP, *Russ. Geol. Geophys.,* 2016, vol. 57, no. 1, pp. 241–258.

Kiselev, A.I., Gordienko, I.V., and Lashkevich, V.V., Petrographic aspects of gravitational instability of tectonically thickened lithosphere, *Tikhookean. Geol.,* 2004, vol. 23, no. 2, pp. 20–29.

Kovach, V.P., Sal'nikova, E.B., Rytsk, E.Yu., et al., The time length of formation of the Angara–Vitim batholith: results of U–Pb geochronological studies, *Dokl. Earth Sci.*, 2012, vol. 444, no. 1, pp. 553–559.

Kovalenko, V.I., Kozlovskii, A.M., and Yarmolyuk, V.V., Trace element ratios as indicators of source mixing and magma differentiation of alkali granitoids and basites of the Haldzan–Buregtey Massif and the Haldzan–Buregtey rare-metal deposit, Western Mongolia, *Petrology,* 2009, vol. 17, no. 2, pp. 158–177.

Kröner, A., Fedotova, A.A., Khain, E.V., et al., Neoproterozoic ophiolite and related high-grade rocks of the Baikal–Muya belt, Siberia: geochronology and geodynamic implications, *J. Asian Earth Sci.,* 2015, vol. 111, pp. 138–160.

Liégeois, J.P., Navez, J., Hertogen, J., and Black, R., Contrasting origin of post-collisional high-K calk-alkaline and shoshonitic versus alkaline and peralkaline granitoids. The use of sliding normalization, *Lithos,* 1998, vol. 45, pp. 1–28.

Litvinovsky, B.A. and Zanvilevich, A.N., Trends of chemical variations of granitoid and basic magmas during evolution of the Mongol–Transbaikalian mobile belt, *Geol. Geofiz.,* 1998, vol. 39, no. 2, pp. 157–177.

Litvinovsky, B.A., Zanvilevich, A.N., Alakshin, A.M., and Podladchikov, Yu.Yu., *Angaro-Vitimskii batolit - krupneishii granitoidnyi pluton* (Angara–Vitim Batholith: The Largest Granitoid Pluton), Novosibirsk: OIGGM SO RAN, 1993.

Litvinovsky, B.A., Zanvilevich, A.N., and Kalmanovich, M.A., Multiple mixing of coexisting syenite and basite magmas and its petrological significance, Ust'-Khilok Massif, Transbaikalia, *Petrologiya,* 1995, vol. 3, no. 2, pp. 133–157.

Litvinovsky, B.A., Posokhov, V.F., and Zanvilevich, A.N., New Rb-Sr age data on the Late Paleozoic granitoids of Western Transbaikalia, *Geol. Geofiz.,* 1999, vol. 40, no. 5, pp. 694–702.

Litvinovsky B.A., Yarmolyuk V.V., Vorontsov A.A., et al., late Triassic stage of formation of the Mongolo–Transbaikalian alkaline–granitoid province: data of isotope-geochemicla studies, *Russ. Geol. Geophys.,* 2001, vol. 42, no. 3, pp. 445–455.

Litvinovsky, B.A., Jahn, B.M., Zanvilevich, A.N., et al., Petrogenesis of syenite–granite suite from Bryansky Complex (Transbaikalia, Russia): implications for the origin of A-type granitoid magmas, *Chem. Geol.,* 2002, vol. 189, pp. 105–133.

Litvinovsky, B.A., Tsygankov, A.A., Jahn, B.M., et al., Origin and evolution of overlapping calc-alkaline and alkaline magmas: the Late Paleozoic post-collisional igneous province of Transbaikalia, *Lithos,* 2011, vol. 125, pp. 845–874.

Litvinovsky, B.A., Zanvilevich, A.N., and Katzir, Y., Formation of composite dykes by contact remelting and magma mingling: the Shaluta Pluton, Transbaikalia (Russia), *J. Asian Earth Sci.,* 2012, vol. 60, pp. 18–30.

Magmaticheskie gornye porody (Magmatic Igneous Rocks), Moscow: Nauka, vol. 3, 1985.

Minina, O.R. Early Hercynides of the Baikal–Vitim Folded Area: Composition, Structure, Geodynamic Evolution, *Extended Abstract of Candidate (Geol.-Min.) Dissertation,* Irkutsk: IZK SO RAN, 2014. 36 pp.

Nédélec, A., Stephens, W.E., and Fallick, A.E., The Panafrican stratoid granites of Madagaskar; alkaline magmatism in a post-collisional setting, *J. Petrol.,* 1995, vol. 36, pp. 1367–1391.

Puffer, J.H., A reactivated back-arc source for camp magma, The Central Atlantic Magmatic Province: insights from fragments of Pangea, *Geophys. Monogr. Amer. Geophys. Union,* 2003, vol. 136, pp. 151–162.

Reichow, M.K., Pringle, M.S., Al'Mukhamedov, A.I., et al., The timing and extent of the eruption of the Siberian traps large igneous province: implications for the end-Permian environmental crisis, *Earth Planet. Sci. Lett.,* 2009, vol. 277, pp. 9–20.

Reichow, M.K., Litvinovsky, B.A., Parrish, R.R., and Saunders, A.D., Multi-stage emplacement of alkaline and peralkaline syenite–granite suites in the Mongolian–Transbaikalian belt, Russia: evidence from U–Pb geochronology and whole rock geochemistry, *Chem. Geol.,* 2010, vol. 273, pp. 120–135.

Reif, F.G., *Fiziko-khimicheskie usloviya formirovaniya krupnykh granitoidnykh mass Vostochnogo Pribaikal'ya* (Physicochemical Conditions of Formation of Large Granitoid Masses of Eastern Baikal Region), Novosibirsk: Nauka, 1976.

Rudnick, R.L. and Gao, S., Composition of the continental crust, in *Treatise on Geochemistry,* Elsevier: Oxford, 2003, vol. 3, pp. 1–64.

Ruzhentsev, S.V., Minina, O.R., Nekrasov, G.E., et al., The Baikal–Vitim Fold System: Structure and Geodynamic Evolution, *Geotectonics,* 2012, vol. 46, no. 2, pp. 87–110.

Rytsk E.Yu., Kovach V.P., Yarmolyuk V.V., et al., Isotopic structure and evolution of the continental crust in the East Transbaikalian segment of the Central Asian Foldbelt, *Geotectonics,* 2011, vol. 45, no. 5, pp. 349–377.

Rytsk E.Yu., Neimark L.A., Amelin Yu.V. Paleozoic granitoids in the northern part of the Baikalian orogenic area: age and past geodynamic settings, *Geotectonics,* 1998, vol. 32, no. 5, 379–393.

Salop, L.I., *Geologiya Baikal'skoi gornoi oblasti* (Geology of the Baikal Mountain Area), Moscow: Nedra, 1967, vol. 2.

Sláma, J., Košler, J., Condon, D.J., et al., Plesovice zircon—a new natural reference material for U–Pb and Hf isotopic microanalysis, *Chem. Geol.,* 2008, vol. 249, pp. 1–35.

Sun, S.S. and McDonough, W.F., Chemical and isotopic systematics of oceanic basalts: implications for mantle com-

position and processes, in *Magmatism in the Oceanic Basins,* Saunders, A.D. and Norry, M.J., Ed.s, *Geol. Soc. Spec. Publ,* 1989, no. 42, pp. 313–345.

Suvorov, V.D., Mishenkina, Z.M., Petrick, G.V., et al., Structure of the crust in the Baikal Rift zone and adjacent areas from deep seismic sounding data, *Tectonophysics,* 2002, vol. 351, pp. 61–74.

Sylvester, P.J., Post-collisional strongly peraluminous granites, *Lithos,* 1998, vol. 45, pp. 29–44.

Titov A.V., Litvinovsky, B.A., Zanvilevich, A.N., and Shadaev, M.G., Hybridization in the composite basite–leucogranite dikes of the Ust'-Khilok Massif (Transbaikalia), *Geol. Geofiz.,* 2000, vol. 41, no. 2, pp. 1714–1728.

Tsygankov, A.A., *Magmaticheskaya evolyutsiya Baikalo-Muiskogo vulkanoplutonicheskogo poyasa v pozdnem dokembrii* (Magmatic Evolution of the Baikal–Muya Volcanoplutonic Belt in the Late Precambrian), Novosibirsk: SO RAN, 2005.

Tsygankov, A.A., Late Paleozoic granitoids in Western Transbaikalia: sequence of formation, sources of magmas, and geodynamics, *Russ. Geol. Geophys.,* 2014, vol. 55, no. 2, pp. 153–176.

Tsygankov, A.A., Burdukov, I.V., and Vrublevskaya, T.T., Composition and genesis of inner-contact syenites of the Khasurta quartz syenite–monzonite massif, Western Transbaikalia, *Petrology,* 2007a, vol. 15, no. 2, 184–209.

Tsygankov, A.A., Matukov, D.I., Berezhnaya, N.G., et al., Late Paleozoic granitoids of Western Kamchatka: magma sources and stages of formation, *Russ. Geol. Geophys.,* 2007b, vol. 48, no. 1, pp. 120–140.

Tsygankov, A.A., Litvinovskii, B.A., Jahn, B.M., et al., Sequence of magmatic events in the late Paleozoic of Transbaikalia, Russia (U–Pb isotope data), *Russ. Geol. Geophys.,* 2010, vol. 51, no. 9, pp. 972–994.

Tsygankov, A.A., Udoratina O.V., Burmakina G.N., and Grove, M., New data on U–Pb dating of zircons and the problem of the duration of the Angara–Vitim granitoid batholith formation, *Dokl. Earth Sci.,* 2012, vol. 447, no. 1, pp. 1273–1277.

Tsygankov, A.A., Udoratina, O.V., Burmakina, G.N., et al., The Early Paleozoic basite magmatism of Western Transbaikalia: composition, isotope age (U–Pb, SHRIMP RG), magma sources, and geodynamics, *Petrology,* 2016a, vol. 24, no. 4, pp. 367–391.

Tsygankov, A.A., Khubanov, V.B., Travin, A.V., et al., Late Paleozoic gabbroids of Western Transbaikalia: U–Pb and Ar–Ar isotopic ages, composition, and petrogenesis, *Russ. Geol. Geophys.,* 2016b, vol. 57, no. 5, pp. 1005–1027.

Turutanov, E.Kh., 3D model of the Angara–Vitim Batholith, in *Geodinamicheskaya evolyutsiya litosfery Tsentral'no-Aziatskogo podvizhnogo poyasa (ot okeana k kontinentu). Materialy soveshchan.* (Geodynamic Evolution of the Lithosphere of the Central Asian Mobile Belt: from an Ocean to Continent, Proceedings of Conference), 2007, vol. 5, no. 2, pp. 131–132.

Valley, J.W., Kinny, P.D., Schulze, D.J., and Spicuzza, M.J., Zircon megacrysts from kimberlite: oxygen isotope heterogeneity among mantle melts, *Contrib. Mineral. Petrol.,* 1998, vol. 133, pp. 1–11.

Whalen, J.B., Currie, K.L., and Chappell, B.W., A-type granites: geochemical characteristics, discrimination and petrogenesis, *Contrib. Mineral. Petrol.,* 1987, vol. 95, pp. 407–419.

Whalen, J.B., McNicoll, V.J., van Staal, C.R., et al., Spatial, temporal and geochemical characteristics of Silurian collision-zone magmatism, Newfoundland Appalachians: an example of a rapidly evolving magmatic system related to slab break-off, *Lithos,* 2006, vol. 89, pp. 377–404.

Wickham, S.M., Litvinovsky, B.A., Zanvilevich, A.N., and Bindeman, I.N., Geochemical evolution of Phanerozoic magmatism in Transbaikalia, East Asia: a key constraint of the origin of K-rich silicic magmas and the process of cratonization, *J. Geophys. Res.,* 1995, 100/B8, pp. 15641–15654.

Wiedenbeck, M., Allé, P., Corfu, F., et al., Three natural zircon standards for U–Th–Pb, Lu–Hf, trace element and REE analyses, *Geostand. Newslett.,* 1995, vol. 19, pp. 1–23.

Xu, Y.G., Wei, X., Luo, Z.Y., et al., The Early Permian Tarim large igneous province: main characteristics and a plume incubation model, *Lithos,* 2014, vol. 204, pp. 20–35.

Yarmolyuk V.V., Budnikov S.V., Kovalenko V.I. et al., Geochronology and geodynamic setting of the Angara–Vitim Batholith, *Petrology,* 1997, vol. 5, no. 5, pp. 401–414.

Yarmolyuk, V.V., Kovalenko, V.I., Sal'nikova E.B., et al., Tectono-magmatic zoning, magma sources, and geodynamics of the Early Mesozoic Mongolia–Transbaikal Province, *Geotectonics,* 2002, vol. 36, no. 4, pp. 293–311.

Yarmolyuk, V.V., Kuzmin, M.I., Kozlovsky, A.M., Late Paleozoic–Early Mesozoic within-plate magmatism in North Asia: traps, rifts, giant batholiths, and the geodynamics of their origin, *Petrology,* 2013, Vol. 21, no. 2, pp. 101–126.

Yarmolyuk, V.V., Kuzmin, M.I., and Ernst, R.E., Late Paleozoic–Early Mesozoic within-plate magmatism in North Asia: traps, rifts, giant batholiths, and the geodynamics of their origin, *J. Asian Earth Sci.,* 2014, vol. 93, pp. 101–126.

Yarmolyuk, V.V., Kozlovskii, A.M., and Kuzmin, M.I., Zoned magmatic areas and anorogenic batholiths formation in the Central Asian orogenic belt (by the example of the late Paleozoic Khangai magmatic area), *Russ. Geol. Geophys.,* 2016, vol. 57, no. 3, pp. 457–475.

Zhao, X.-F., Zhou, M.L., Li, J.-W., and Wu, F.-Y., Association of Neoproterozoic A-type and I-type granites in south China: implications for generation of A-type granites in a subduction-related environment, *Chem. Geol.,* 2008, vol. 257, pp. 1–15.

Zonenshain, L.P., Kuzmin M.I., Natapov, L.M., *Tektonika litosfernykh plit territorii SSSR* (Tectonics of Lithospheric Plates of the USSR Territory), Moscow: Nedra, 1990, vol. 1–2.

Zorin, Yu.A., Geodynamics of the western part of the Mongolia–Okhotsk collisional belt, Trans-Baikal region (Russia) and Mongolia, *Tectonophysics,* 1999, vol. 306, pp. 33–56.

Translated by E. Kurdyukov